

# Chapter 4

## Image Enhancement in the Frequency Domain



## 4.1 Background

- 2-D transform can be applied to image enhancement, restoration, encoding, and description.
- Fourier transform (FT)
  - Fourier's idea – [fig. 4.1](#).

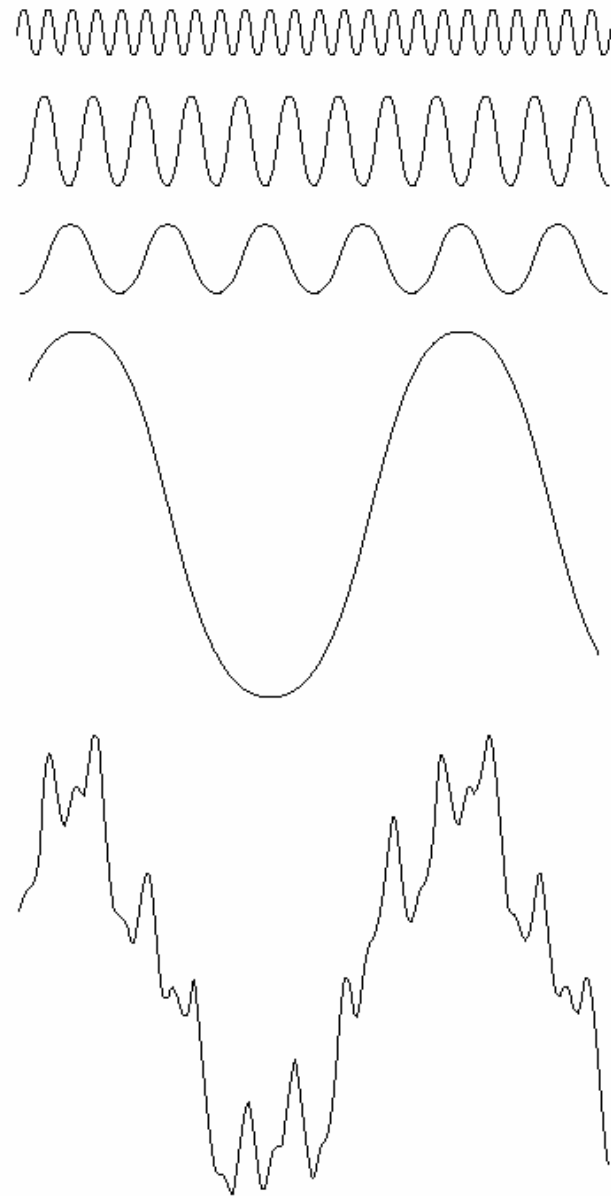
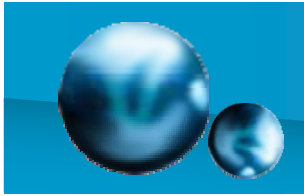


**FIGURE 4.1** The function at the bottom is the sum of the four functions above it. Fourier's idea in 1807 that periodic functions could be represented as a weighted sum of sines and cosines was met with skepticism.



## 4.2 Introduction to the Fourier transform

- © Let  $f(x)$  be a continuous function of a real variable  $x$ . The Fourier transform of  $f(x)$ , denoted as  $\mathfrak{F}\{f(x)\}$ , is defined by

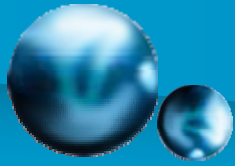
$$\mathfrak{F}\{f(x)\} = F(u) = \int_{-\infty}^{\infty} f(x) \exp[-j2\pi ux] dx$$

where  $j = \sqrt{-1}$

- © Given  $F(u)$ ,  $f(x)$  can be obtained by using inverse Fourier transform

$$\mathfrak{F}^{-1}\{F(u)\} = f(x) = \int_{-\infty}^{\infty} F(u) \exp[j2\pi ux] du$$

- ©  $f(x)$  is real,  $F(u)$  is complex



## 4.2 Introduction to the Fourier transform

⊙  $F(u) = R(u) + jI(u)$   
 $= |F(u)| e^{j\phi(u)}$

⊙  $\phi(u) = \tan^{-1} \left[ \frac{I(u)}{R(u)} \right]$       ※ phase angle ※

⊙  $|F(u)| = \left[ R^2(u) + I^2(u) \right]^{1/2}$       ※ Fourier spectrum of  $f(x)$  ※

⊙  $P(u) = |F(u)|^2$       ※ power spectrum of  $f(x)$  ※

⊙  $u$  is called the frequency variable

⊙ Fig. 3.1 shows a simple function and its Fourier spectrum

⊙ Let  $f(x,y)$  be a continuous function of two real variables  $x$  and  $y$ .



## 4.2 Introduction to the Fourier transform

### Example 1

$$F(u) = \int_{-\infty}^{\infty} f(x) \exp[-j2\pi ux] dx$$

$$= \int_0^x A \exp[-j2\pi ux] dx$$

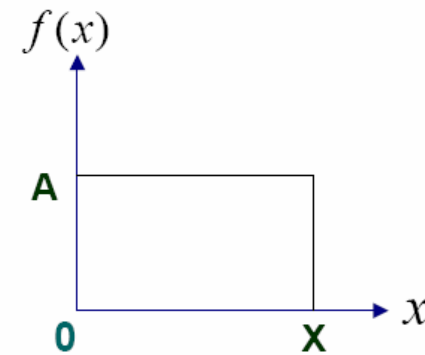
$$= \frac{-A}{j2\pi u} \left[ \exp(-j2\pi ux) \right]_0^x = \frac{-A}{j2\pi u} \left[ \exp(-j2\pi ux) - 1 \right]$$

$$= \frac{A}{j2\pi u} \left[ \exp(j\pi ux) - \exp(-j\pi ux) \right] \exp(-j\pi ux)$$

$$= \frac{A}{\pi u} \sin(\pi ux) \exp(-j\pi ux)$$

$$|F(u)| = \left| \frac{A}{\pi u} \sin(\pi ux) \right| \left| \exp(-j\pi ux) \right| = AX \left| \frac{\sin \pi ux}{\pi ux} \right|$$

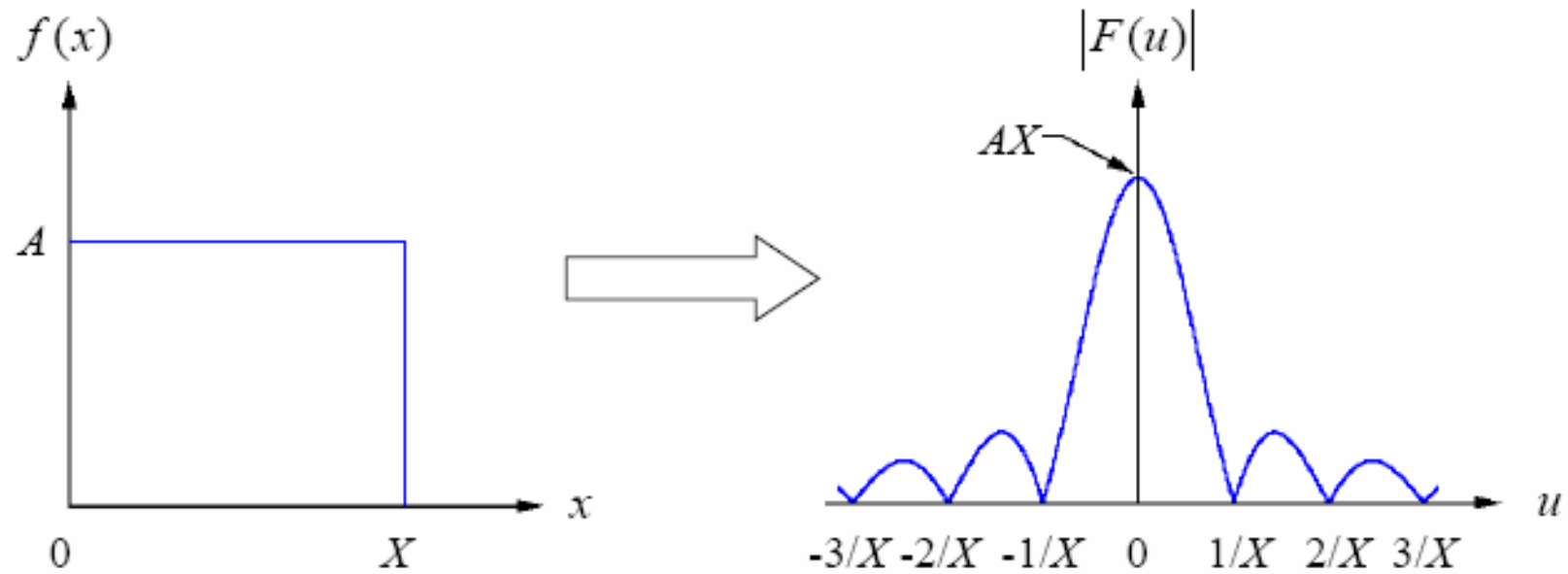
$$= AX |\text{sinc } \pi ux|$$





## 4.2 Introduction to the Fourier transform

✓ Example:





## 4.2 Introduction to the Fourier transform

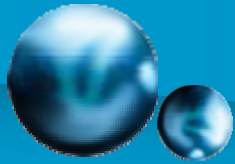
2-D Fourier transform of  $f(x,y)$ , denoted as  $\mathfrak{F}\{f(x,y)\}$ , is defined by

$$\mathfrak{F}\{f(x,y)\} = F(u,v) = \int_{-\infty}^{\infty} \int_{-\infty}^{\infty} f(x,y) \exp[-j2\pi(ux + vy)] dx dy$$

© Given  $F(u,v)$ ,  $f(x,y)$  can be obtained by using inverse Fourier transform

$$\mathfrak{F}^{-1}\{F(u,v)\} = f(x,y) = \int_{-\infty}^{\infty} \int_{-\infty}^{\infty} F(u,v) \exp[j2\pi(ux + vy)] du dv$$





## 4.2 Introduction to the Fourier transform

$$\begin{aligned}\textcircled{c} F(u,v) &= R(u,v) + jI(u,v) \\ &= |F(u,v)| e^{j\phi(u,v)}\end{aligned}$$

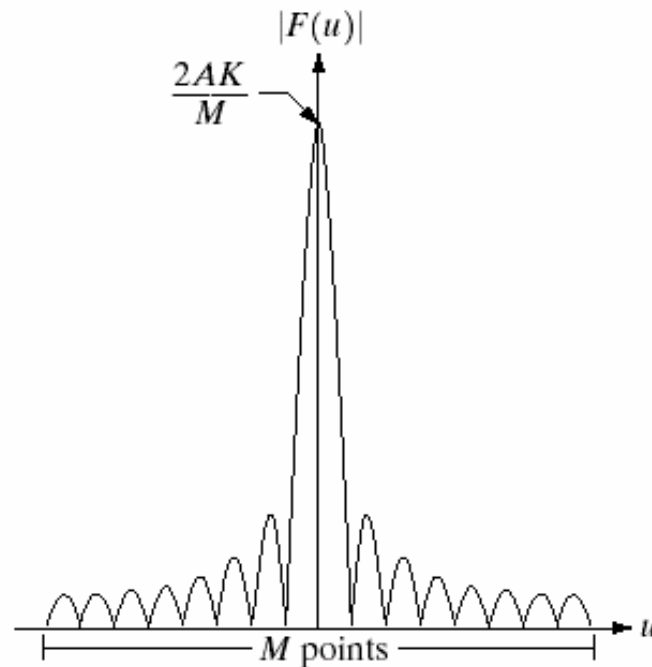
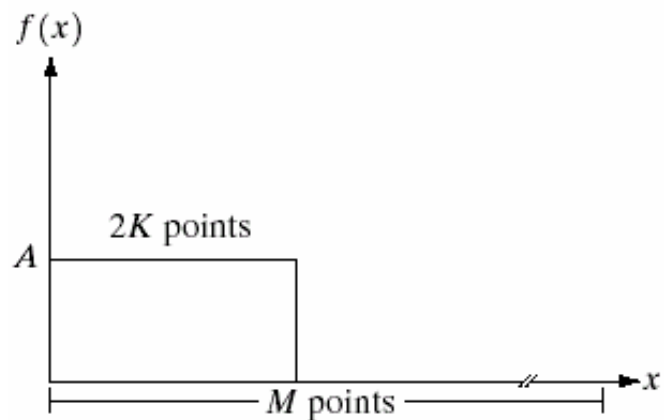
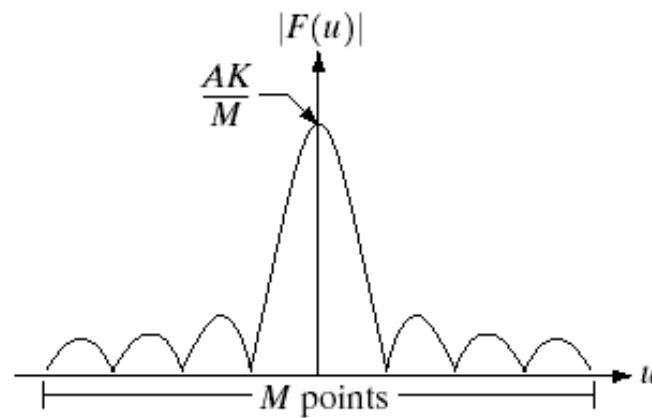
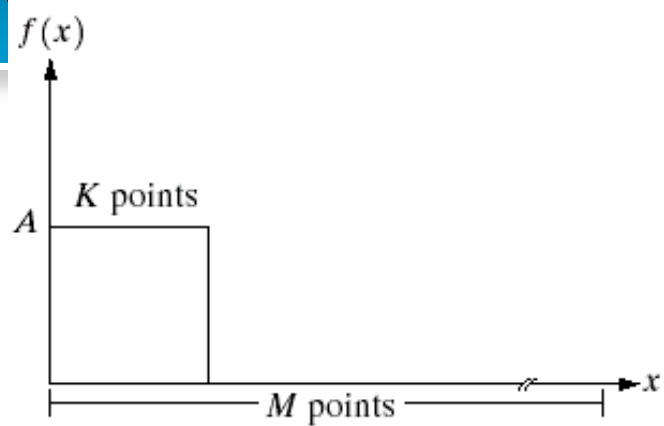
$$\textcircled{c} \phi(u,v) = \tan^{-1} \left[ \frac{I(u,v)}{R(u,v)} \right] \quad \text{※ phase angle ※}$$

$$\textcircled{c} |F(u,v)| = \left[ R^2(u,v) + I^2(u,v) \right]^{1/2} \quad \text{※ Fourier spectrum of } f(x,y) \text{ ※}$$

$$\textcircled{c} P(u,v) = |F(u,v)|^2 \quad \text{※ power spectrum of } f(x,y) \text{ ※}$$

◎ u and v are called the frequency variables

Example 4.1. Fourier spectra of two simple 1-D functions. ([Fig. 4.2](#))

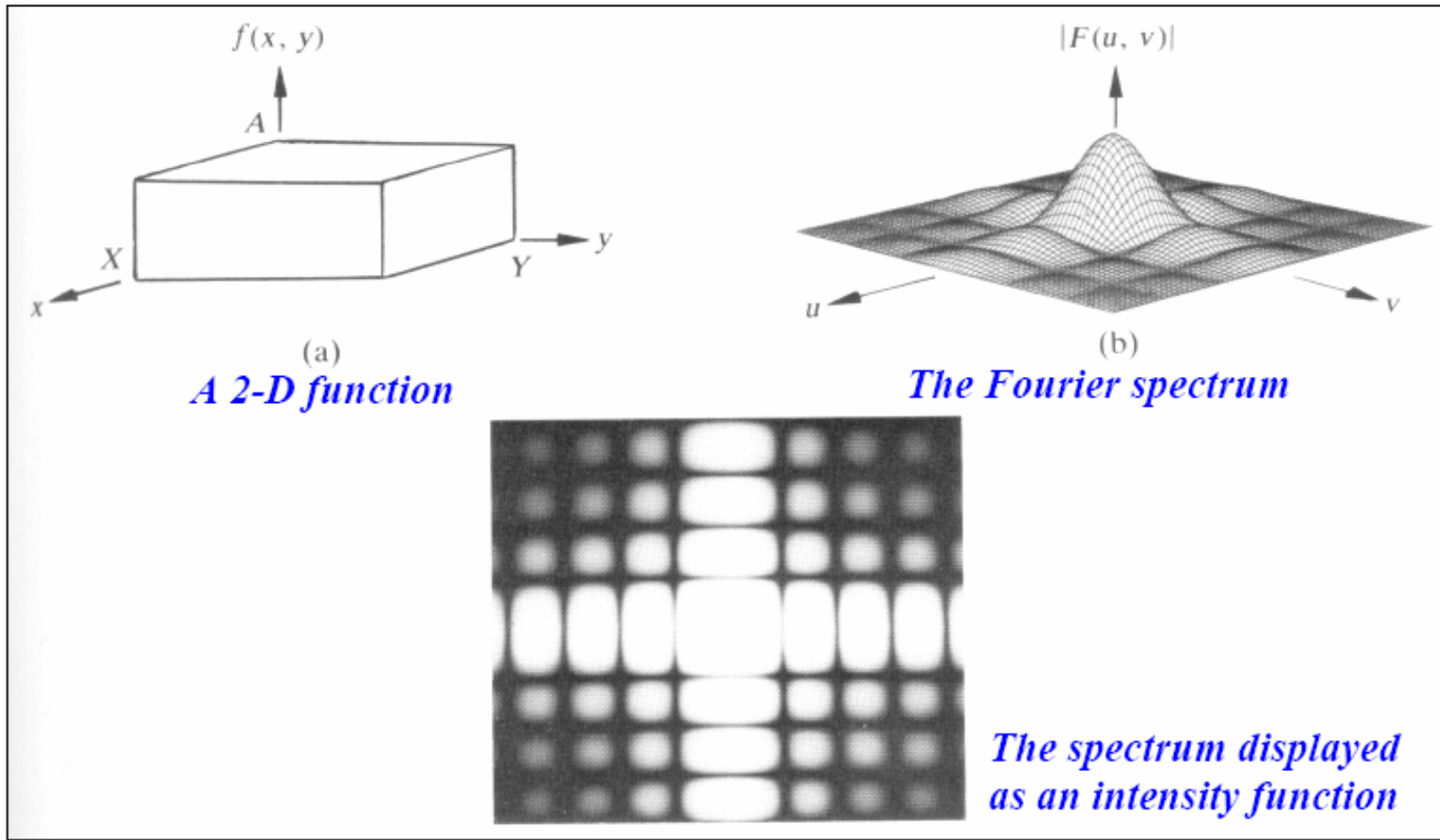


a	b
c	d

**FIGURE 4.2** (a) A discrete function of  $M$  points, and (b) its Fourier spectrum. (c) A discrete function with twice the number of nonzero points, and (d) its Fourier spectrum.



## 4.2 Introduction to the Fourier transform





## 4.2 Introduction to the Fourier transform

- The discrete Fourier transform (DFT)
  - For 1-D transform: Let the sequence  $\{f(0), f(1), \dots, f(N-1)\}$  be  $n$  real points, the discrete Fourier transform pair is given by

$$F(u) = \frac{1}{N} \sum_{x=0}^{N-1} f(x) \exp[-j2\pi ux / N]$$

for  $u=0, 1, 2, \dots, N-1$ , and

$$f(x) = \sum_{u=0}^{N-1} F(u) \exp[j2\pi ux / N]$$

for  $x=0, 1, 2, \dots, N-1$

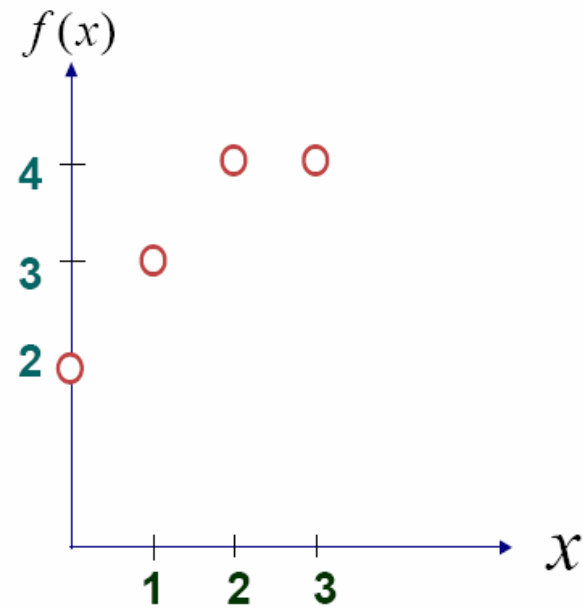
*DFT Exp.*

$$\begin{aligned} F(0) &= \sum_{x=0}^3 f(x) \exp[0] \\ &= [f(0)+f(1)+f(2)+f(3)] \\ &= (2+3+4+4)=13 \end{aligned}$$

$$\begin{aligned} F(1) &= \sum f(x) \exp[-j2\pi x/4] \\ &= 2e^0 + 3e^{-j\frac{\pi}{2}} + 4e^{-j\pi} + 4e^{-j\frac{3\pi}{2}} \\ &= 2-3j-4+4j \\ &= -2+j \end{aligned}$$

$$\begin{aligned} F(2) &= \sum f(x) \exp[-j4\pi x/4] \\ &= 2e^0 + 3e^{-j\pi} + 4e^{-j2\pi} + 4e^{-j3\pi} \\ &= 2-3+4-4=-1 \end{aligned}$$

$$F(3) = -2-j$$





## 4.2 Introduction to the Fourier transform

- For 2-D transform: in the two-variable case the discrete Fourier transform pair is

$$F(u,v) = \frac{1}{N} \sum_{x=0}^{N-1} \sum_{y=0}^{N-1} f(x,y) \exp[-j2\pi(ux + vy) / N]$$

for  $u,v = 0,1,2,\dots,N-1$ , and

$$f(x,y) = \frac{1}{N} \sum_{u=0}^{N-1} \sum_{v=0}^{N-1} F(u,v) \exp[j2\pi(ux + vy) / N]$$

for  $x,y = 0,1,\dots,N-1$ .



## 4.2 Introduction to the Fourier transform

(1) A continuous function  $f(x,y)$  is discretized into a sequence

$$\{f(x_0, y_0), f(x_0 + \Delta x, y_0), f(x_0 + \Delta x, y_0 + \Delta y), \dots, f(x_0 + |M-1| \Delta x, y_0 + |N-1| \Delta y)\}$$

(2) Define

$$g(x, y) = f(x_0 + x\Delta x, y_0 + y\Delta y) \quad x = 1, \dots, M-1, \quad y = 1, \dots, N-1$$

(3) The discrete Fourier transform  $G(u,v)$  of  $g(x,y)$  satisfies

$$G(u, v) = F(u\Delta u, v\Delta v) \quad \text{and} \quad \Delta u = \frac{1}{M\Delta x}, \quad \Delta v = \frac{1}{M\Delta y}$$

Example 4.2. Centered spectrum of a simple 2-D functions. ([Fig. 4.3](#))

Example 4.3. Fourier spectrum ([Fig. 4.4](#))

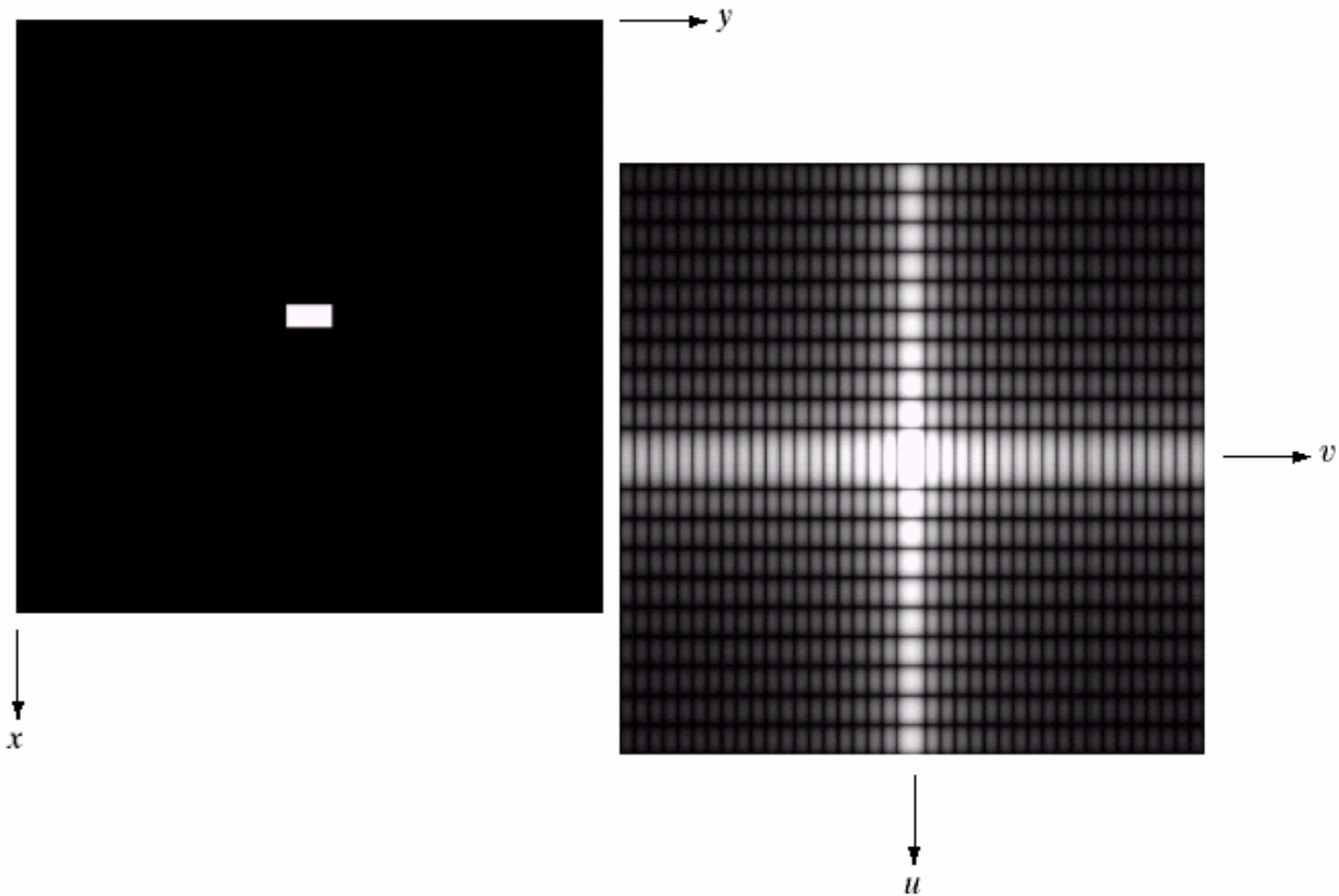


a b

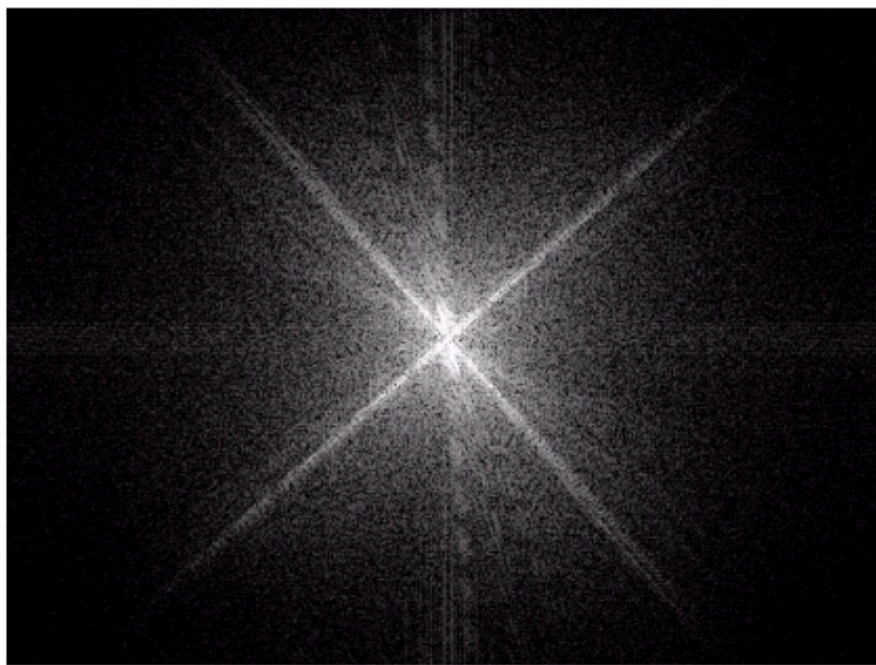
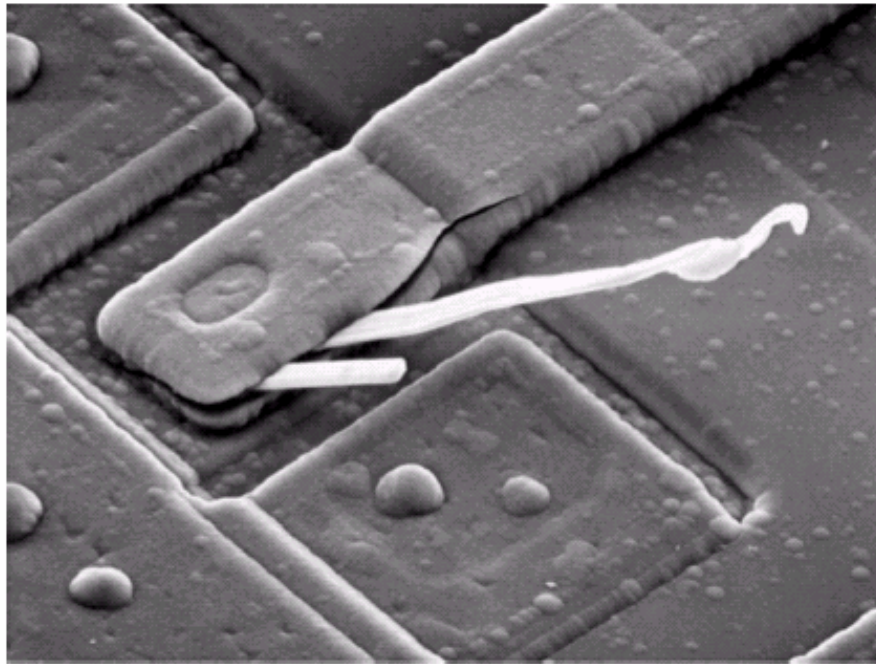
**FIGURE 4.3**

(a) Image of a  $20 \times 40$  white rectangle on a black background of size  $512 \times 512$  pixels.

(b) Centered Fourier spectrum shown after application of the log transformation given in Eq. (3.2-2). Compare with Fig. 4.2.







a  
b

**FIGURE 4.4**

(a) SEM image of a damaged integrated circuit.

(b) Fourier spectrum of (a).

(Original image courtesy of Dr. J. M. Hudak,

Brockhouse Institute for Materials Research,

McMaster University,

Hamilton,

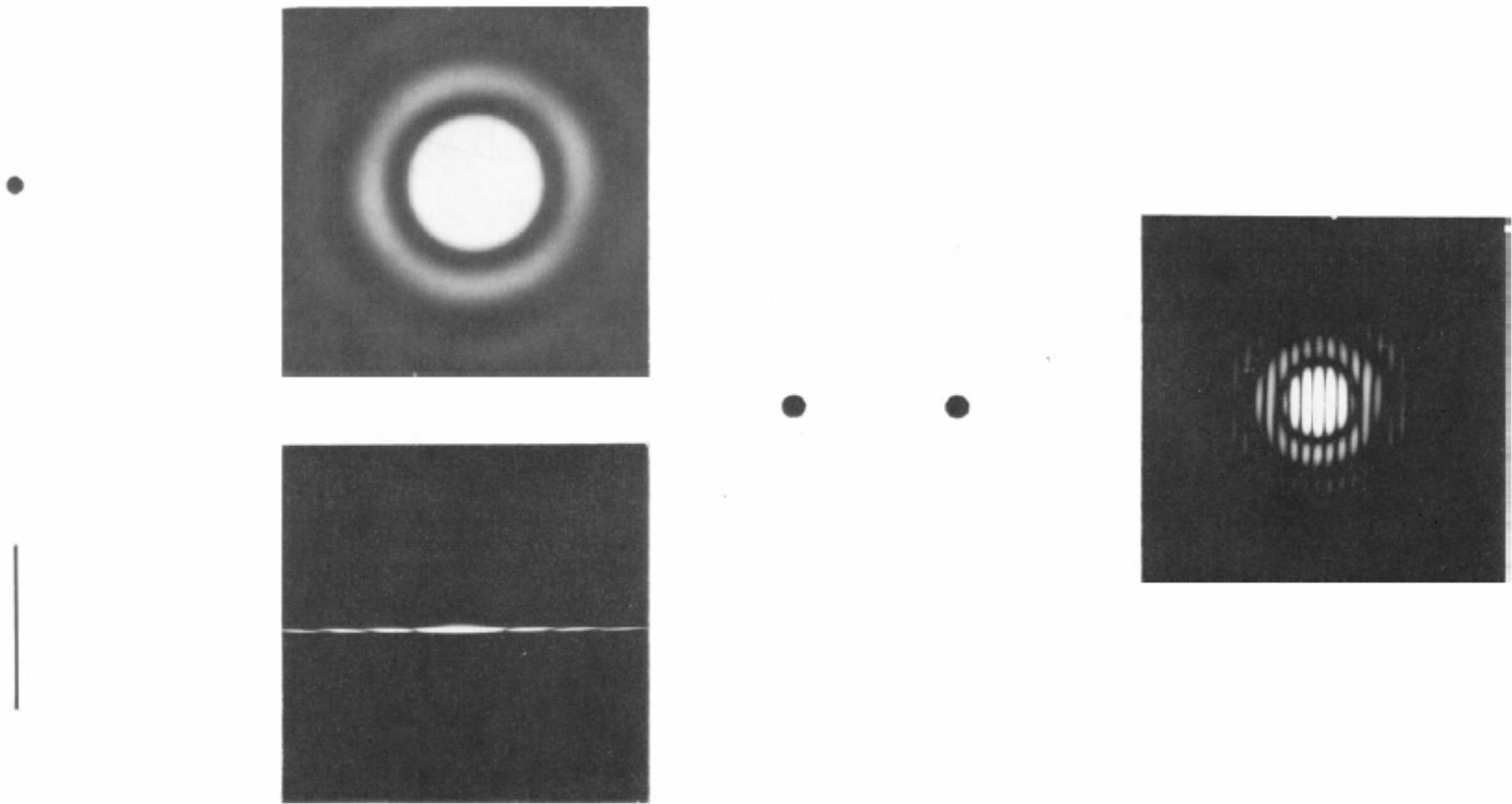
Ontario, Canada.)

---



## 4.2 Introduction to the Fourier transform

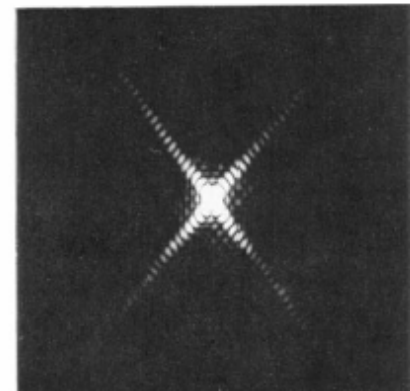
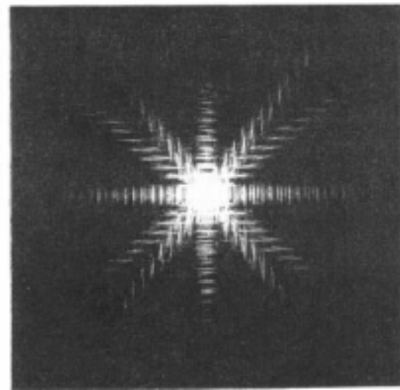
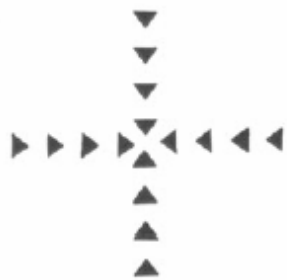
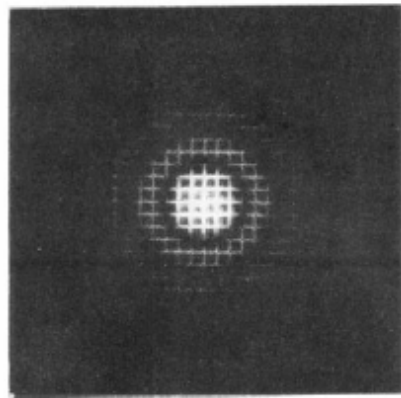
✓ Example:





## 4.2 Introduction to the Fourier transform

✓ Example:





# Filtering in the Frequency Domain

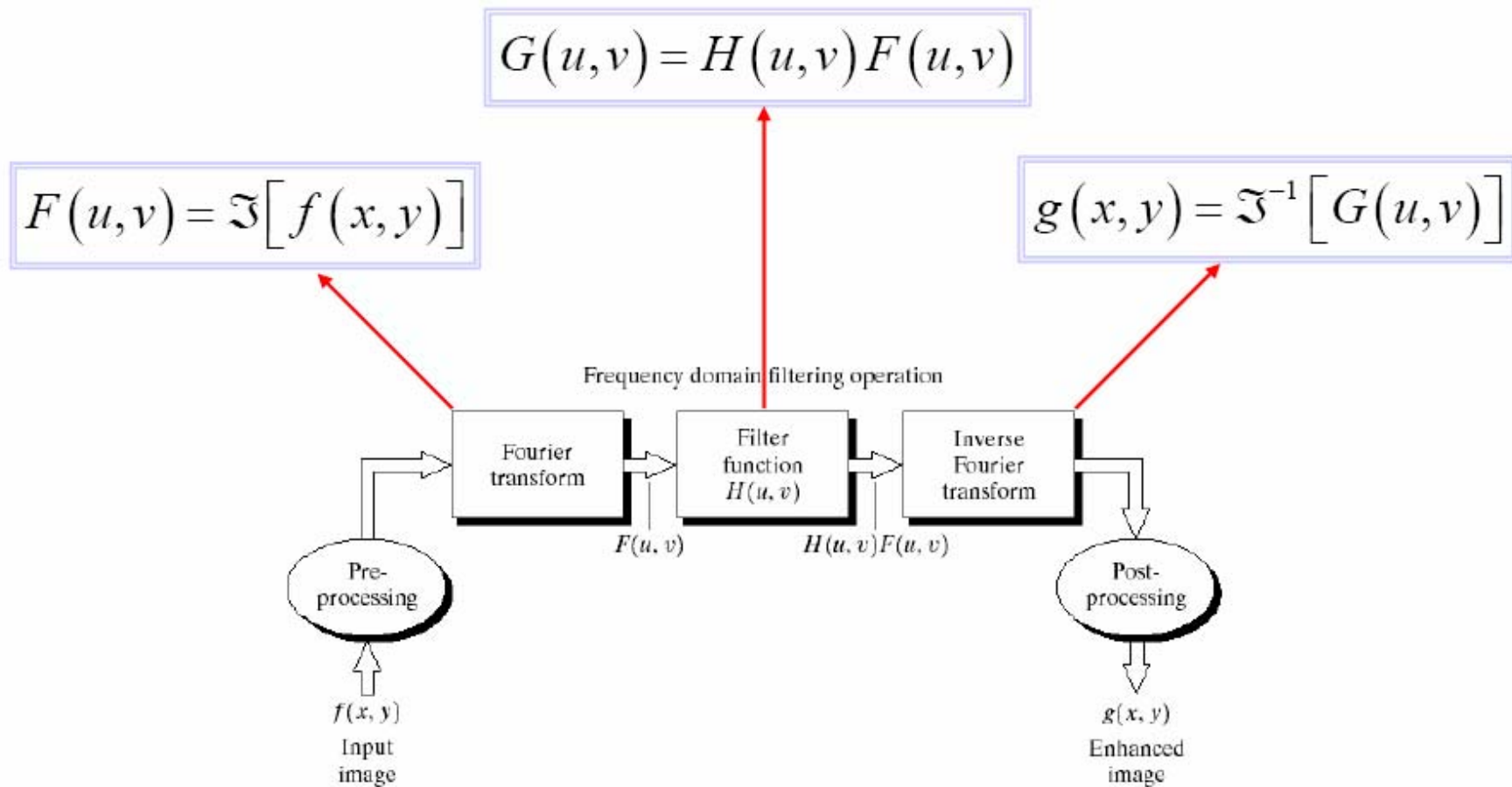


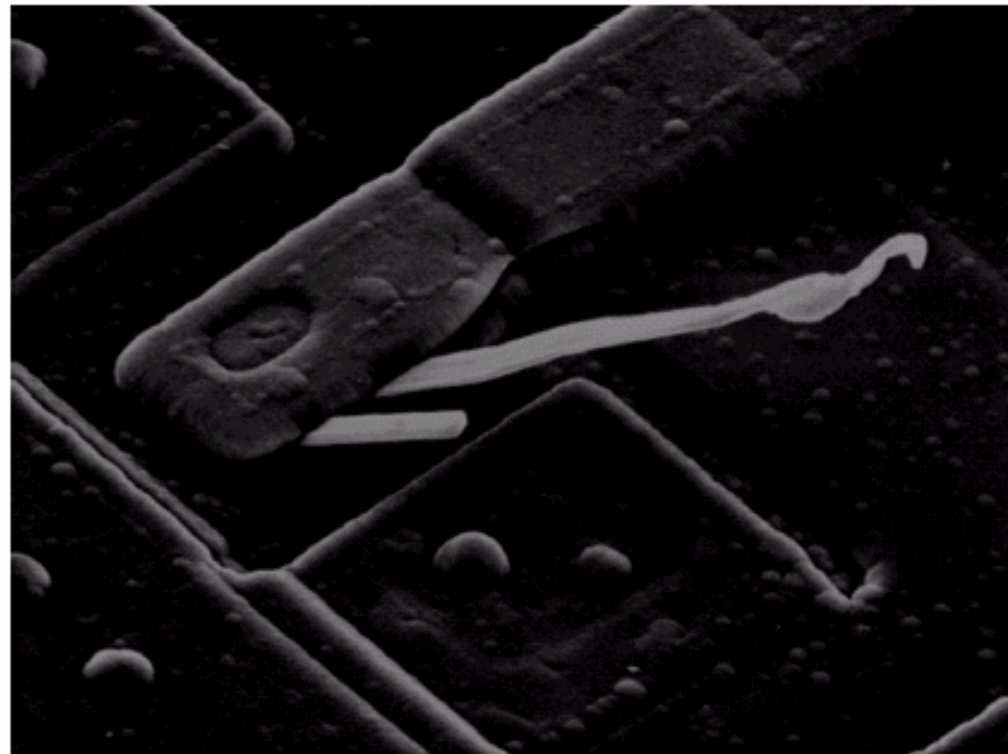
FIGURE 4.5 Basic steps for filtering in the frequency domain.



**FIGURE 4.6**

Result of filtering the image in Fig. 4.4(a) with a notch filter that set to 0 the  $F(0, 0)$  term in the Fourier transform.

---





Relation between average value of a function and its Fourier transform:

$$\bar{f}(x, y) = \frac{1}{N^2} \sum_{x=0}^{N-1} \sum_{y=0}^{N-1} f(x, y)$$

$$F(u, v) = \frac{1}{N} \sum_{x=0}^{N-1} \sum_{y=0}^{N-1} f(x, y) W_N^{ux} W_N^{vy}$$

$$\Rightarrow \bar{f}(x, y) = \frac{1}{N} F(0, 0)$$

# Convolution Theorem

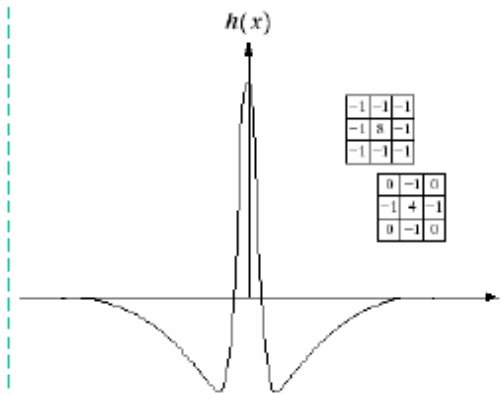
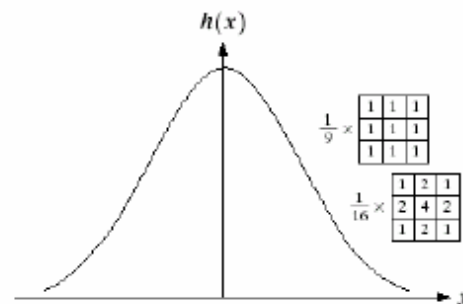
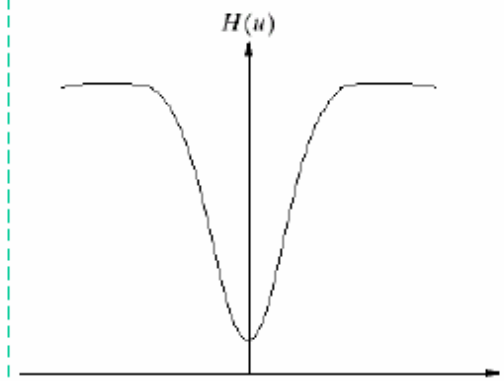
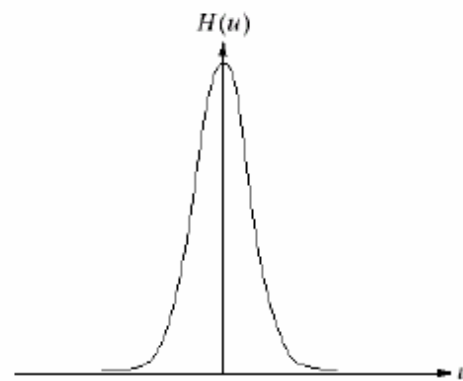
$$f(x, y) * h(x, y) \Leftrightarrow F(u, v)H(u, v)$$

Lowpass

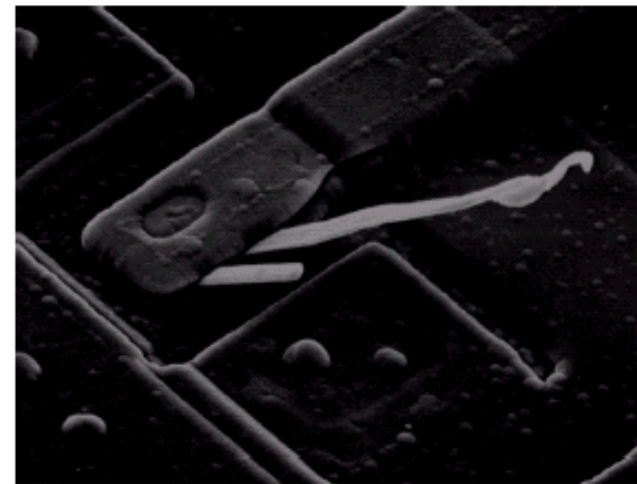
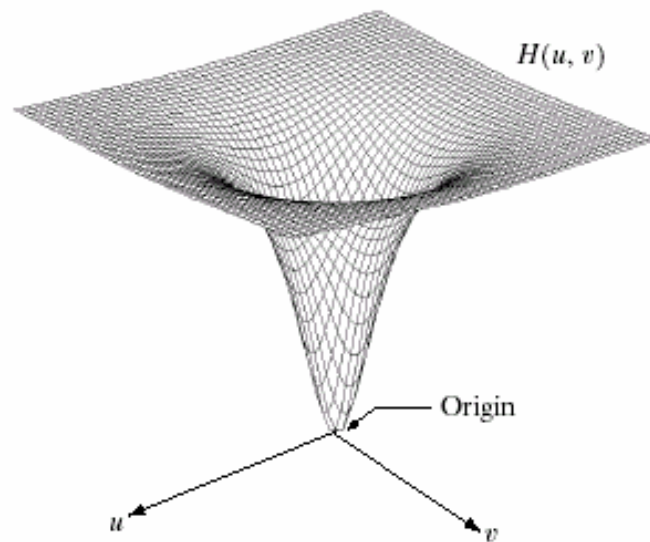
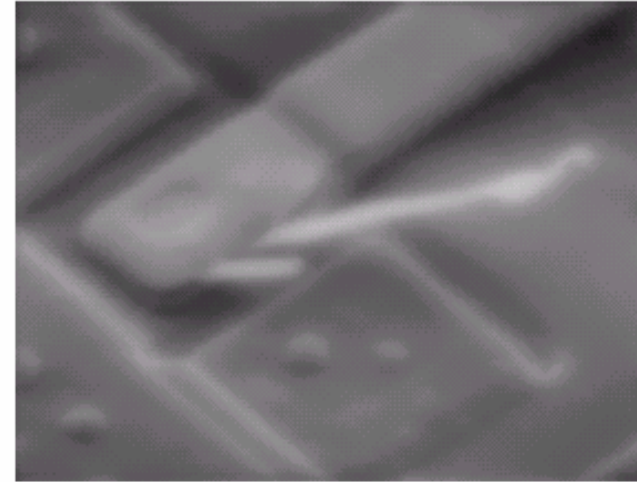
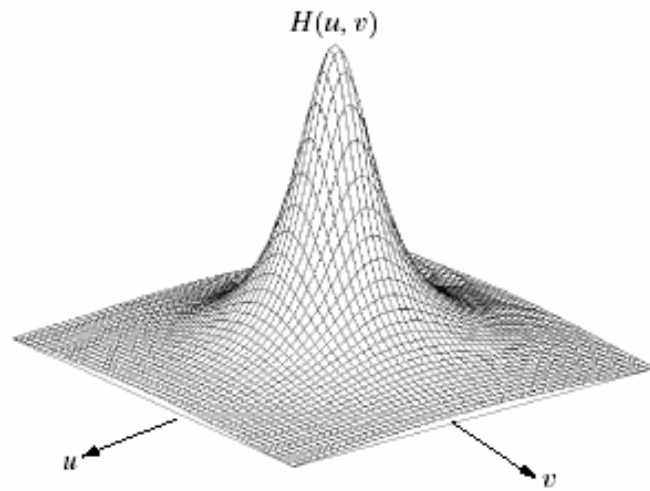
Highpass

Frequency

Spatial



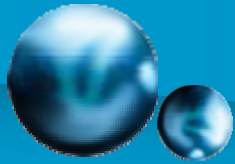




a b  
c d

**FIGURE 4.7** (a) A two-dimensional lowpass filter function. (b) Result of lowpass filtering the image in Fig. 4.4(a). (c) A two-dimensional highpass filter function. (d) Result of highpass filtering the image in Fig. 4.4(a).

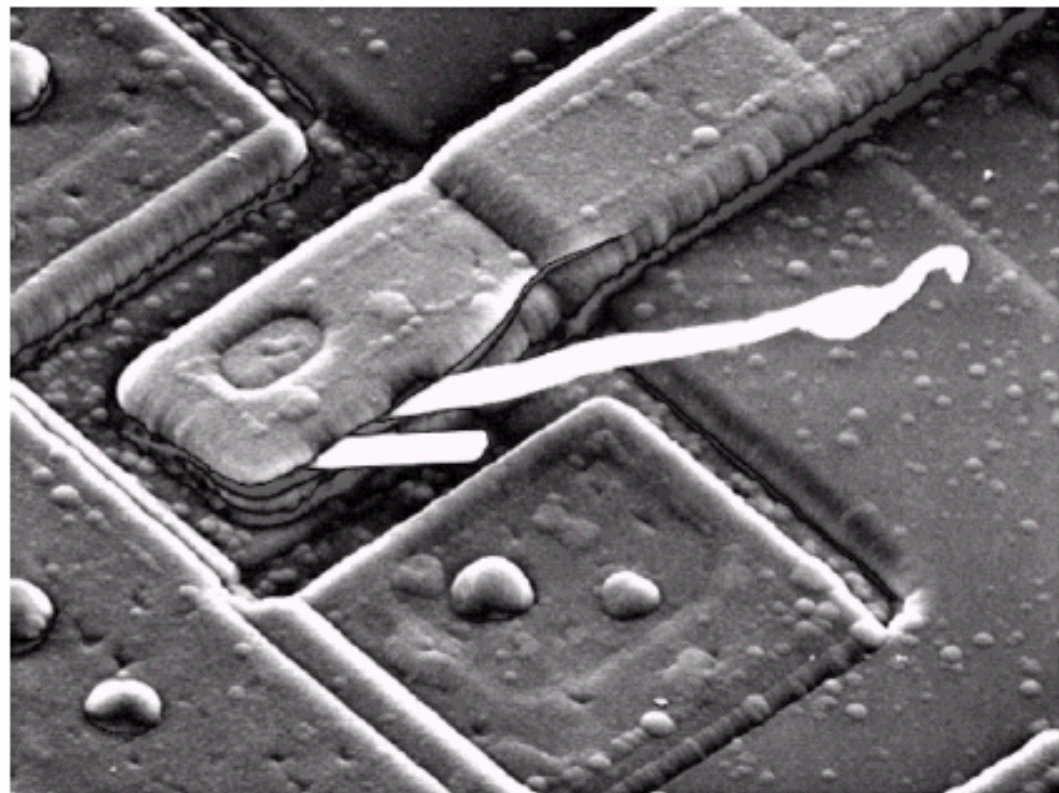


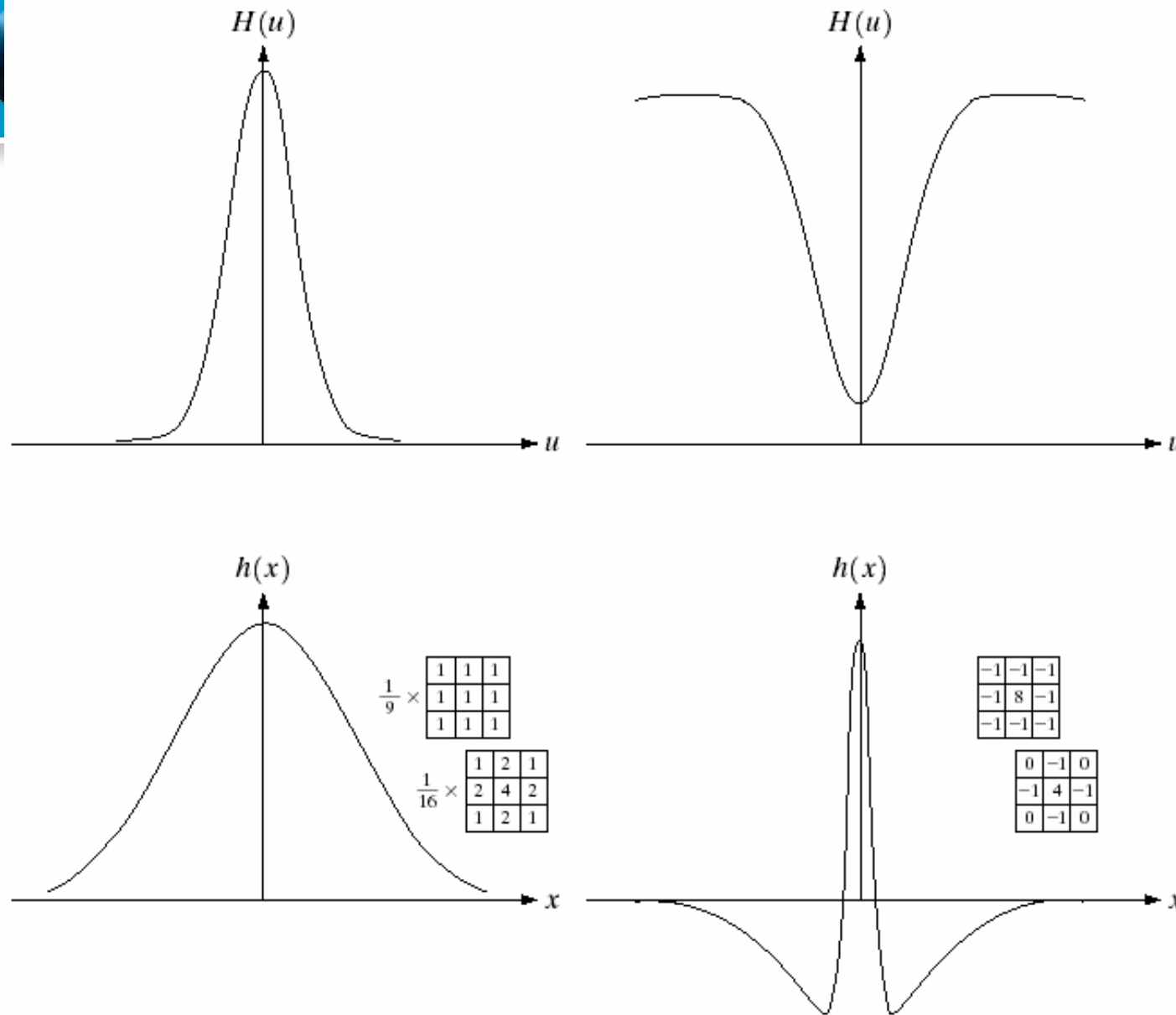


**FIGURE 4.8**

Result of highpass filtering the image in Fig. 4.4(a) with the filter in Fig. 4.7(c), modified by adding a constant of one-half the filter height to the filter function. Compare with Fig. 4.4(a).

---





a b  
c d

**FIGURE 4.9**

(a) Gaussian frequency domain lowpass filter.

(b) Gaussian frequency domain highpass filter.

(c) Corresponding lowpass spatial filter.

(d) Corresponding highpass spatial filter. The masks

shown are used in Chapter 3 for lowpass and highpass filtering.



## 4.3 Smoothing Frequency-Domain Filters

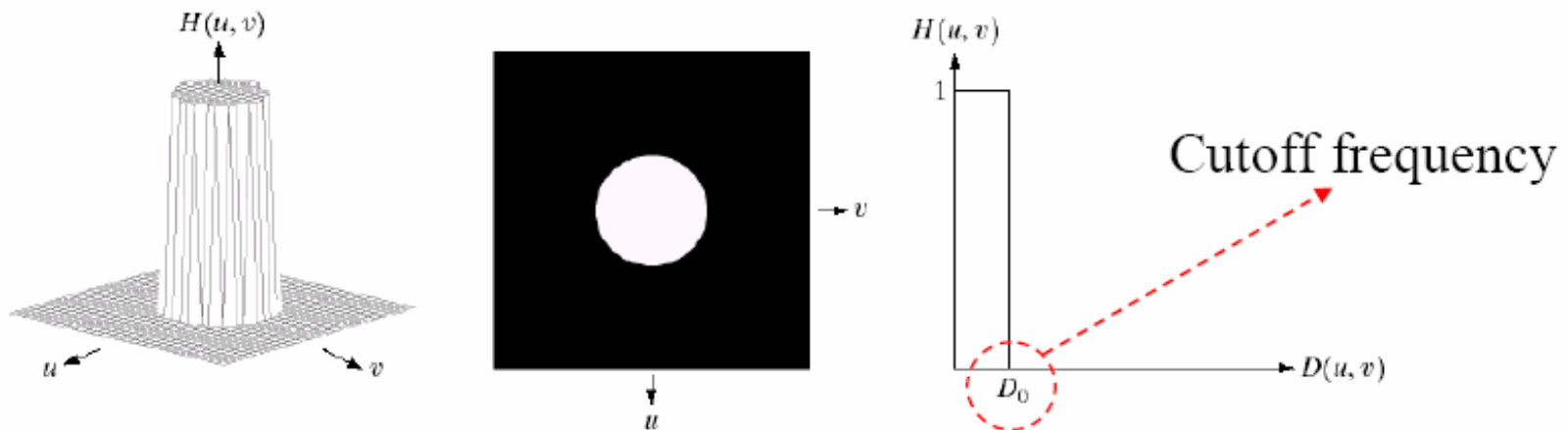
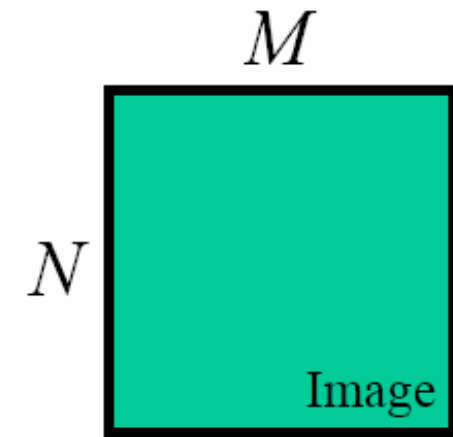
- Ideal lowpass filters (ILPF)
  - [Fig. 4.10](#)
  - Example 4.4. Image power as a function of distance from the origin of the DFT. ([Fig. 4.11](#)) ([Fig. 4.12](#))



# Ideal lowpass filters

$$H(u, v) = \begin{cases} 1 & \text{if } D(u, v) \leq D_0 \\ 0 & \text{if } D(u, v) > D_0 \end{cases}$$

$$D(u, v) = \left[ \left( u - \frac{M}{2} \right)^2 + \left( v - \frac{N}{2} \right)^2 \right]^{1/2}$$



a b c

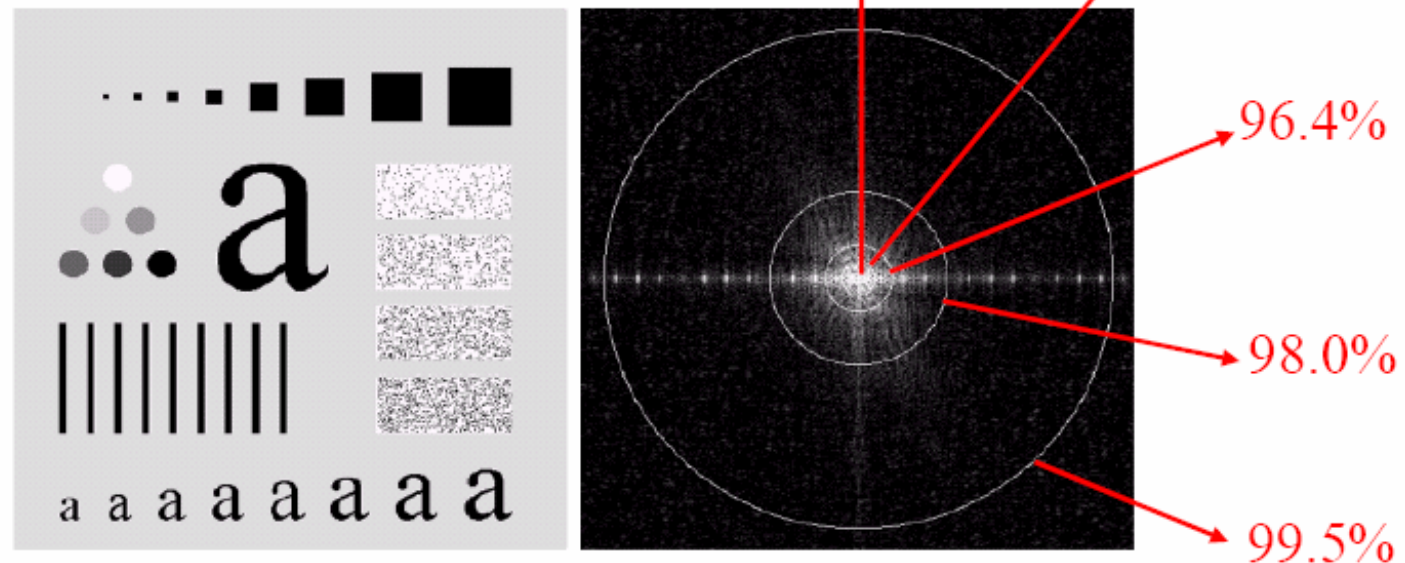
**FIGURE 4.10** (a) Perspective plot of an ideal lowpass filter transfer function. (b) Filter displayed as an image. (c) Filter radial cross section.



## Ideal lowpass filters

$$\text{Total image power : } P_T = \sum_{u=0}^{M-1} \sum_{v=0}^{N-1} P(u, v)$$

$$\text{Enclosed power : } \alpha = 100 \left[ \frac{\sum_u \sum_v P(u, v)}{P_T} \right]$$



a b

**FIGURE 4.11** (a) An image of size  $500 \times 500$  pixels and (b) its Fourier spectrum. The superimposed circles have radii values of 5, 15, 30, 80, and 230, which enclose 92.0, 94.6, 96.4, 98.0, and 99.5% of the image power, respectively.



# Lost power

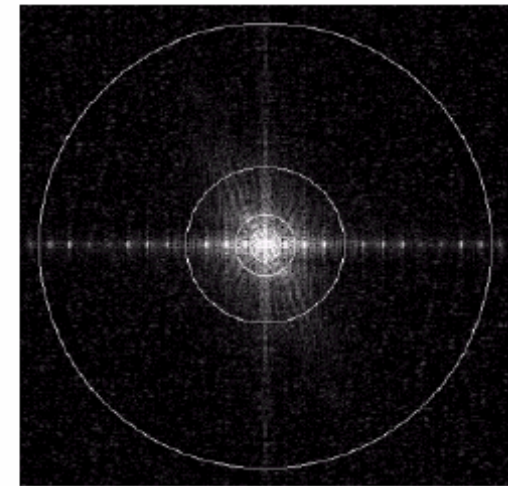
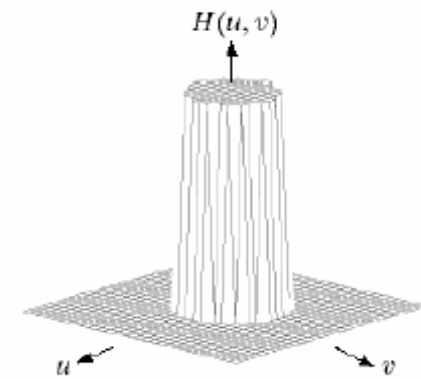
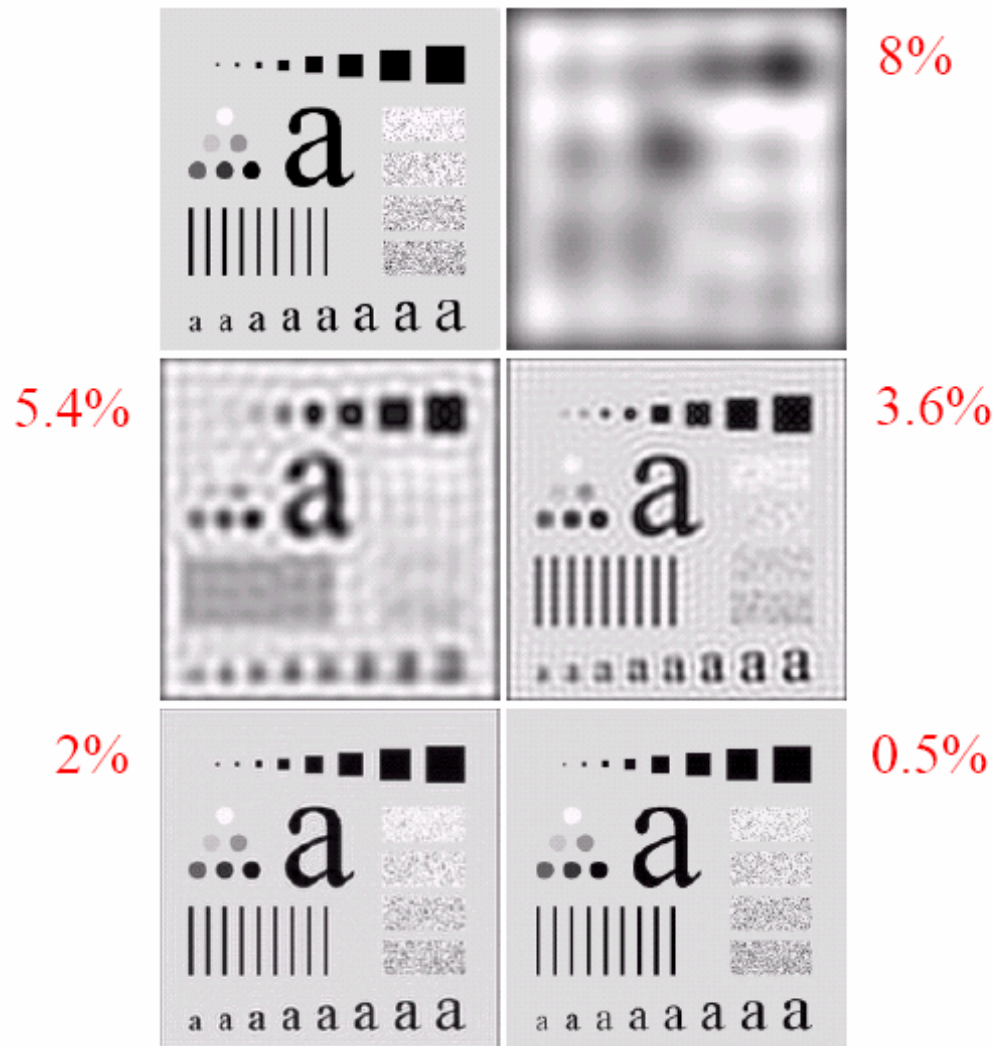


**FIGURE 4.12** (a) Original image. (b)–(f) Results of ideal lowpass filtering with cutoff frequencies set at radii values of 5, 15, 30, 80, and 230, as shown in Fig. 4.11(b). The power removed by these filters was 8, 5.4, 3.6, 2, and 0.5% of the total, respectively.

## ringing and blurring

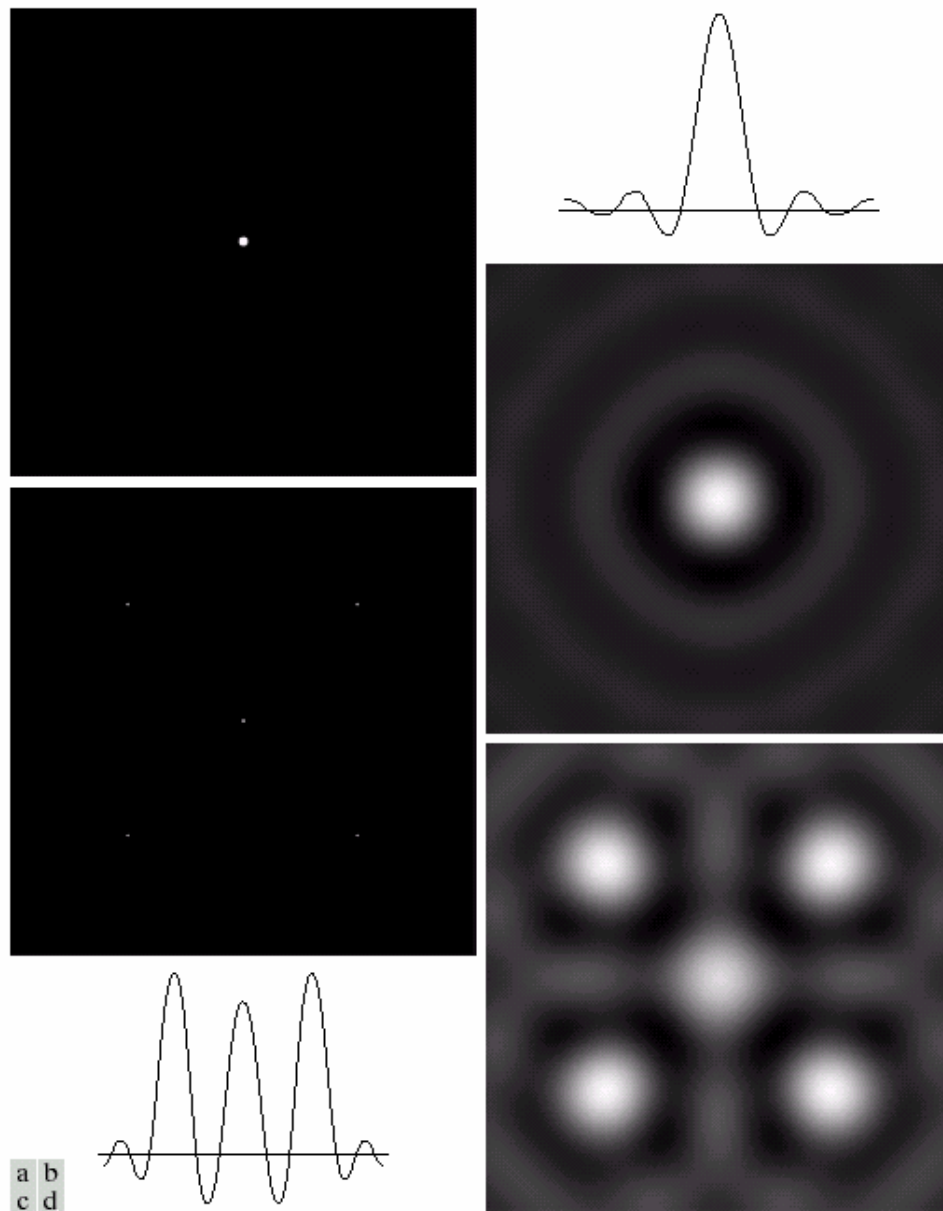


**FIGURE 4.13** (a) A frequency-domain ILPF of radius 5. (b) Corresponding spatial filter (note the ringing). (c) Five impulses in the spatial domain, simulating the values of five pixels. (d) Convolution of (b) and (c) in the spatial domain.



## 4.3 Smoothing Frequency-Domain Filters

- Butterworth lowpass filters (BLPF)
  - Example 4.5. ([Fig. 4.15](#)) ([Fig. 4.16](#))
- Gaussian lowpass filters (GLPFs)
  - Example 4.6. ([Fig. 4.17](#)) ([Fig. 4.18](#)) ([Fig. 4.19](#))
- Additional Examples of Lowpass Filtering
  - [Fig. 4.20](#)
  - [Fig. 4.21](#)



# Butterworth lowpass filters of order $n$

$$H(u, v) = \frac{1}{1 + [D(u, v)/D_0]^{2n}}$$

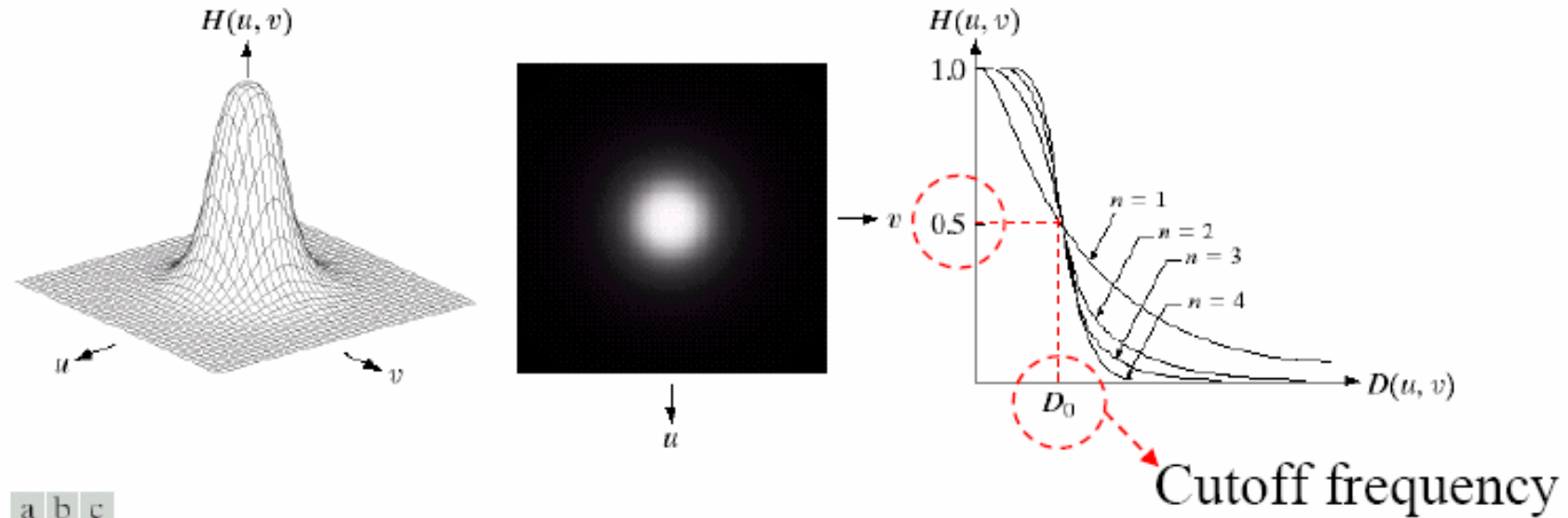
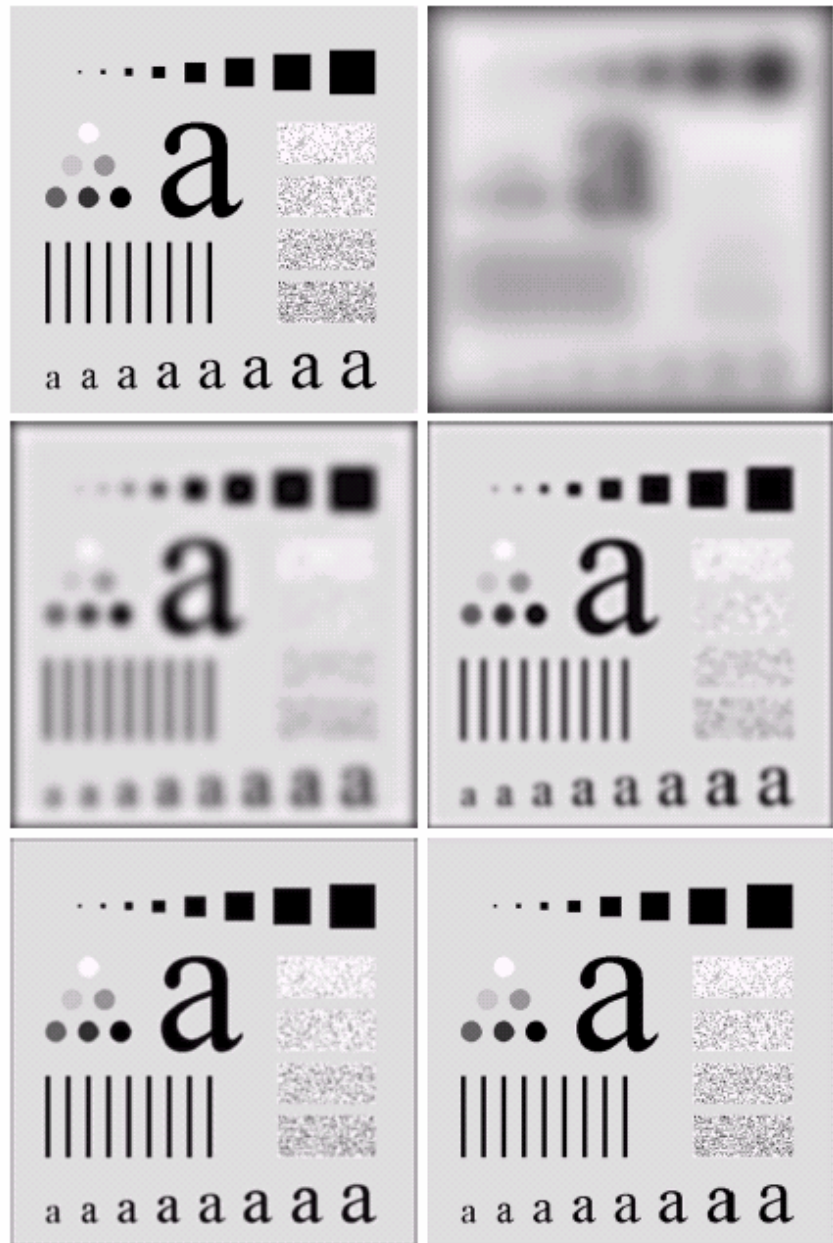
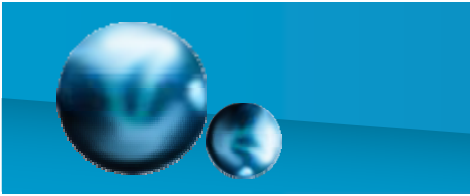
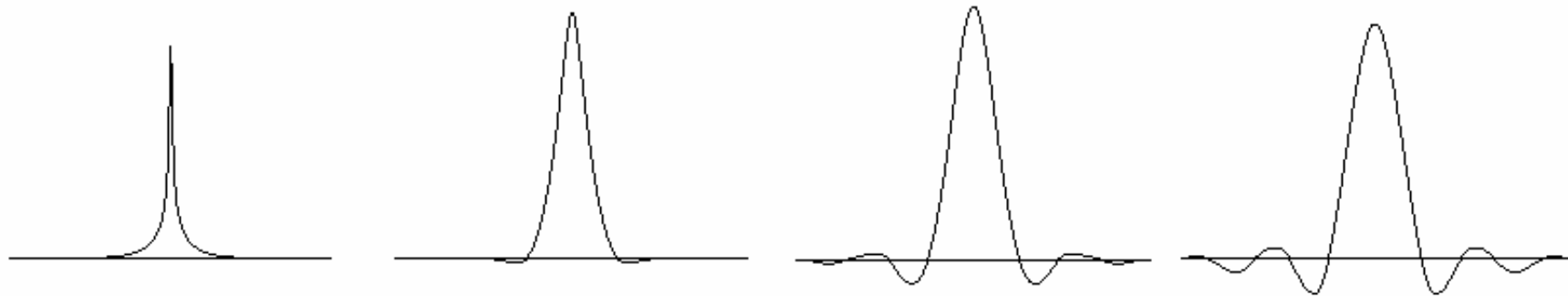
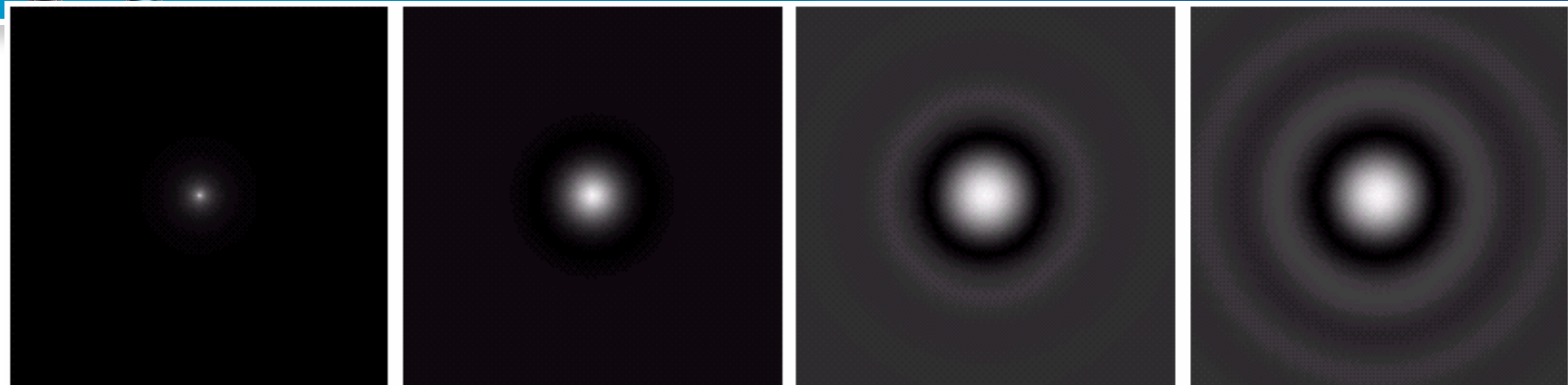


**FIGURE 4.14** (a) Perspective plot of a Butterworth lowpass filter transfer function. (b) Filter displayed as an image. (c) Filter radial cross sections of orders 1 through 4.



a b  
c d  
e f

**FIGURE 4.15** (a) Original image. (b)–(f) Results of filtering with BLPFs of order 2, with cutoff frequencies at radii of 5, 15, 30, 80, and 230, as shown in Fig. 4.11(b). Compare with Fig. 4.12.



a b c d

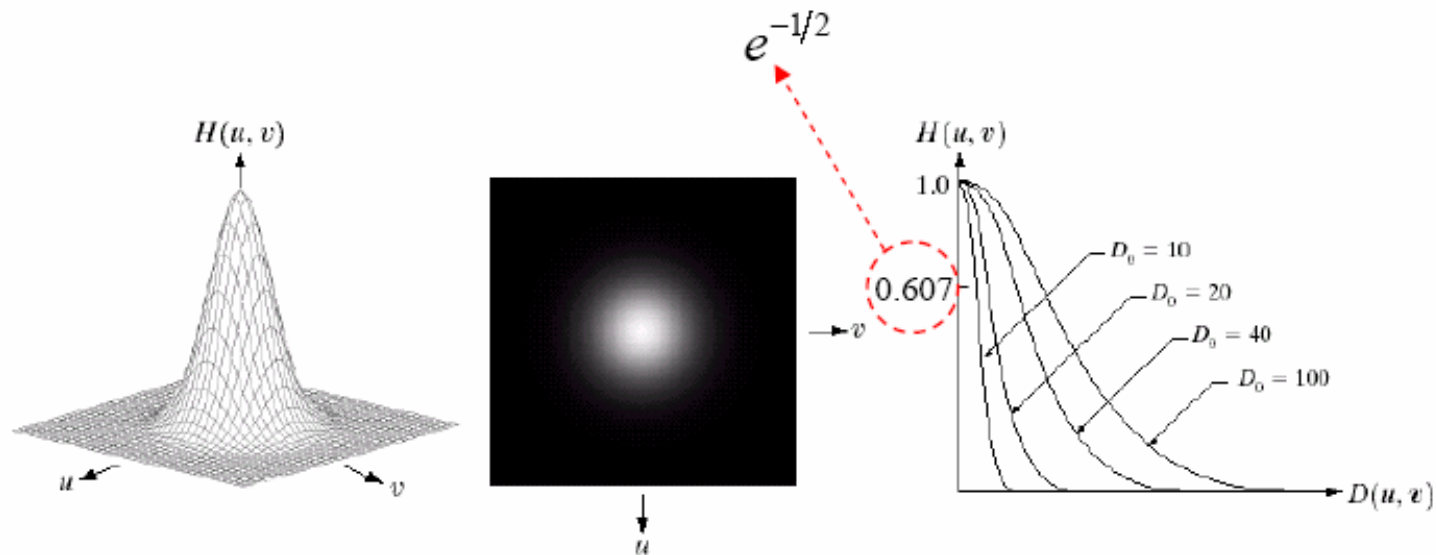
**FIGURE 4.16** (a)–(d) Spatial representation of BLPFs of order 1, 2, 5, and 20, and corresponding gray-level profiles through the center of the filters (all filters have a cutoff frequency of 5). Note that ringing increases as a function of filter order.



# Gaussian Lowpass filters

$$H(u, v) = e^{-D^2(u, v) / 2D_0^2}$$

$D_0$  : Cutoff frequency



a b c

**FIGURE 4.17** (a) Perspective plot of a GLPF transfer function. (b) Filter displayed as an image. (c) Filter radial cross sections for various values of  $D_0$ .

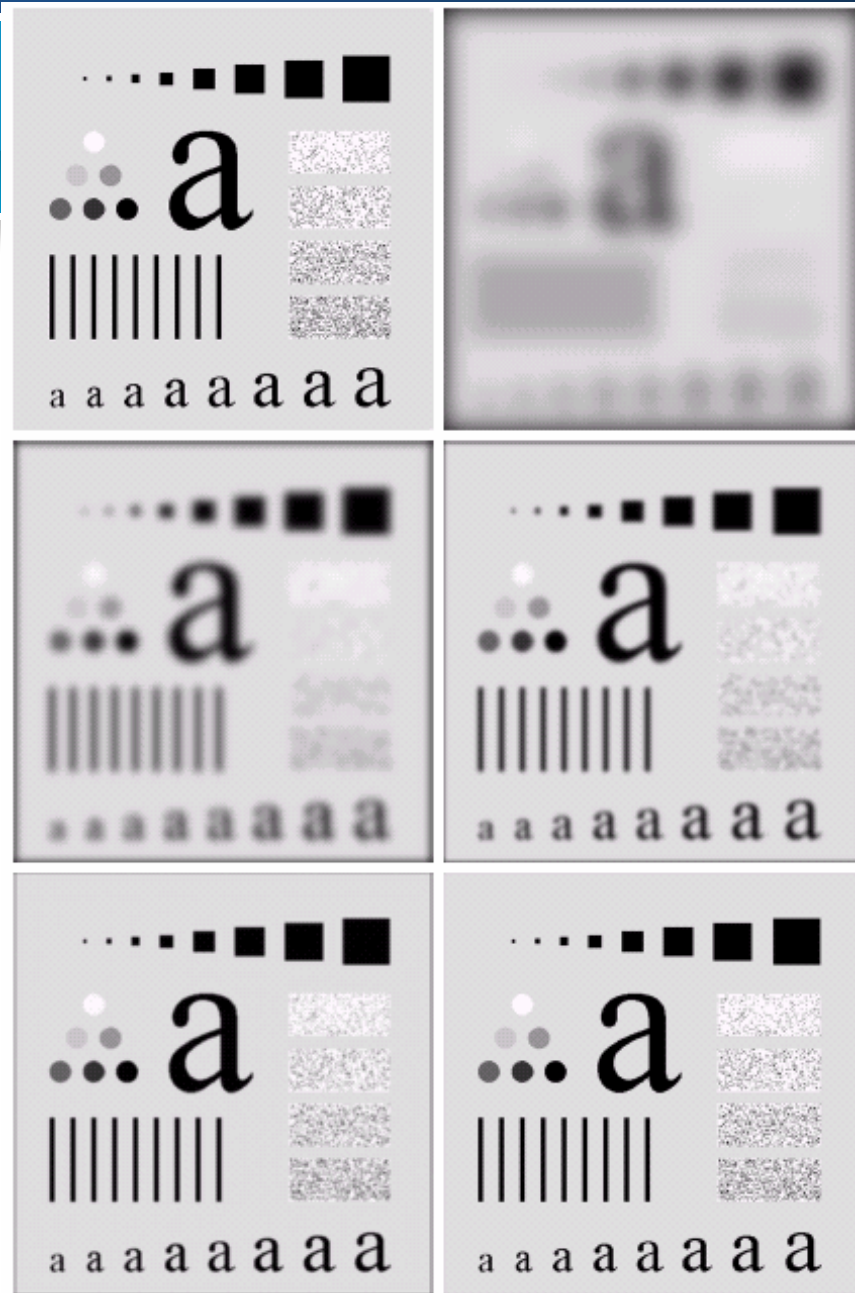


**FIGURE 4.18** (a) Original image. (b)–(f) Results of filtering with Gaussian lowpass filters with cutoff frequencies set at radii values of 5, 15, 30, 80, and 230, as shown in Fig. 4.11(b). Compare with Figs. 4.12 and 4.15.

a b  
c d  
e f



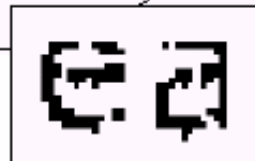
# Character recognition

a b

**FIGURE 4.19**

(a) Sample text of poor resolution (note broken characters in magnified view).  
(b) Result of filtering with a GLPF (broken character segments were joined).

Historically, certain computer programs were written using only two digits rather than four to define the applicable year. Accordingly, the company's software may recognize a date using "00" as 1900 rather than the year 2000.



Historically, certain computer programs were written using only two digits rather than four to define the applicable year. Accordingly, the company's software may recognize a date using "00" as 1900 rather than the year 2000.







a b c

**FIGURE 4.20** (a) Original image ( $1028 \times 732$  pixels). (b) Result of filtering with a GLPF with  $D_0 = 100$ . (c) Result of filtering with a GLPF with  $D_0 = 80$ . Note reduction in skin fine lines in the magnified sections of (b) and (c).



## Reducing the effect of scan lines



a b c

**FIGURE 4.21** (a) Image showing prominent scan lines. (b) Result of using a GLPF with  $D_0 = 30$ . (c) Result of using a GLPF with  $D_0 = 10$ . (Original image courtesy of NOAA.)

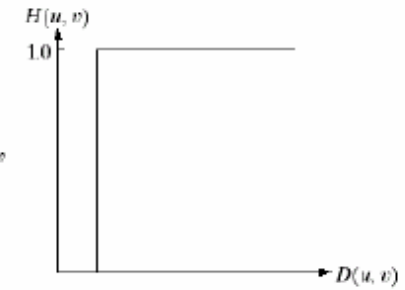
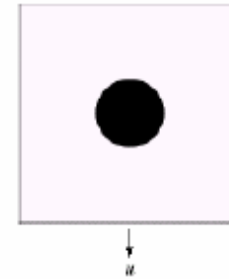
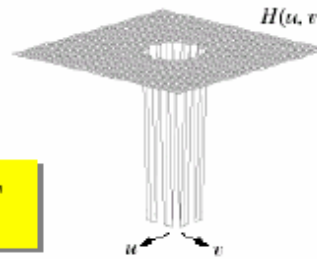




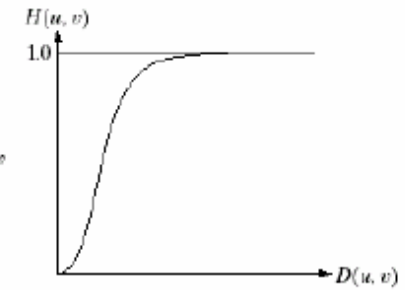
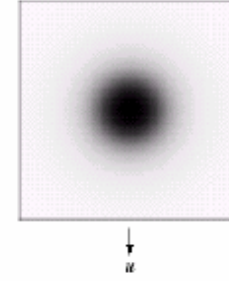
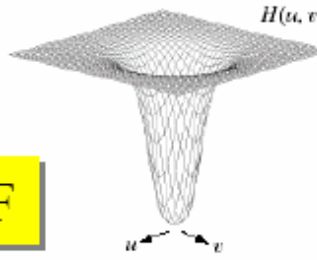
# 4.4 Sharpening Frequency-Domain Filters

$$H_{hp}(u, v) = 1 - H_{lp}(u, v)$$

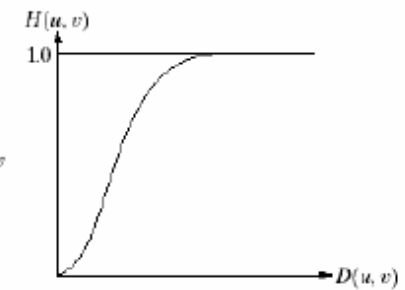
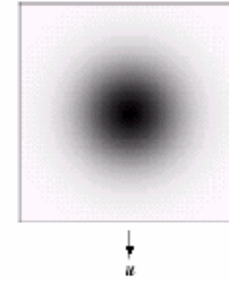
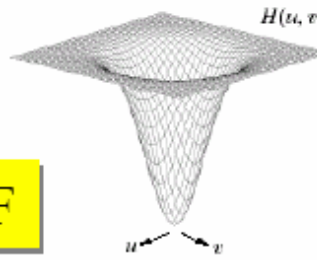
IHPF



BHPF



GHPF



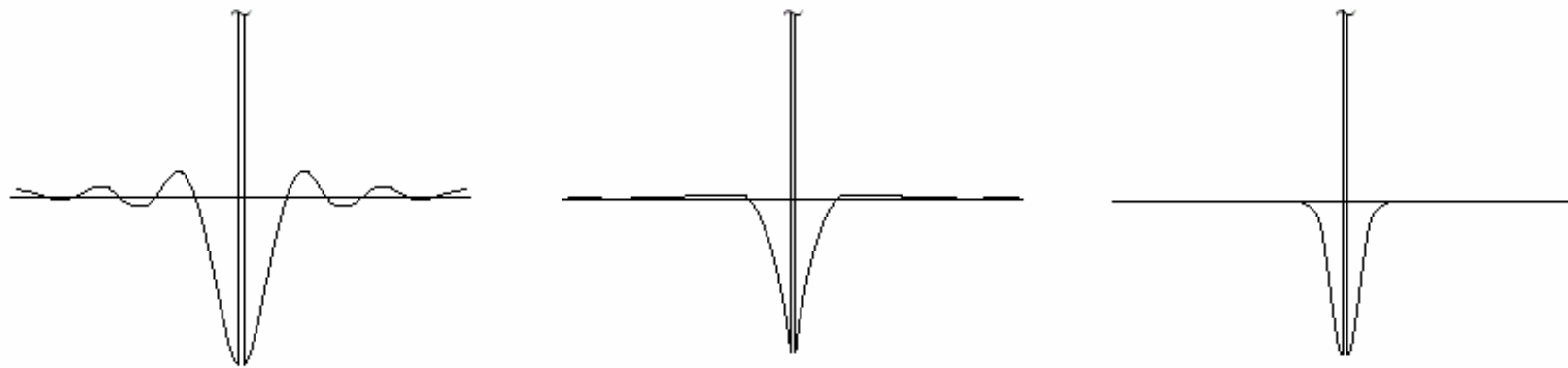
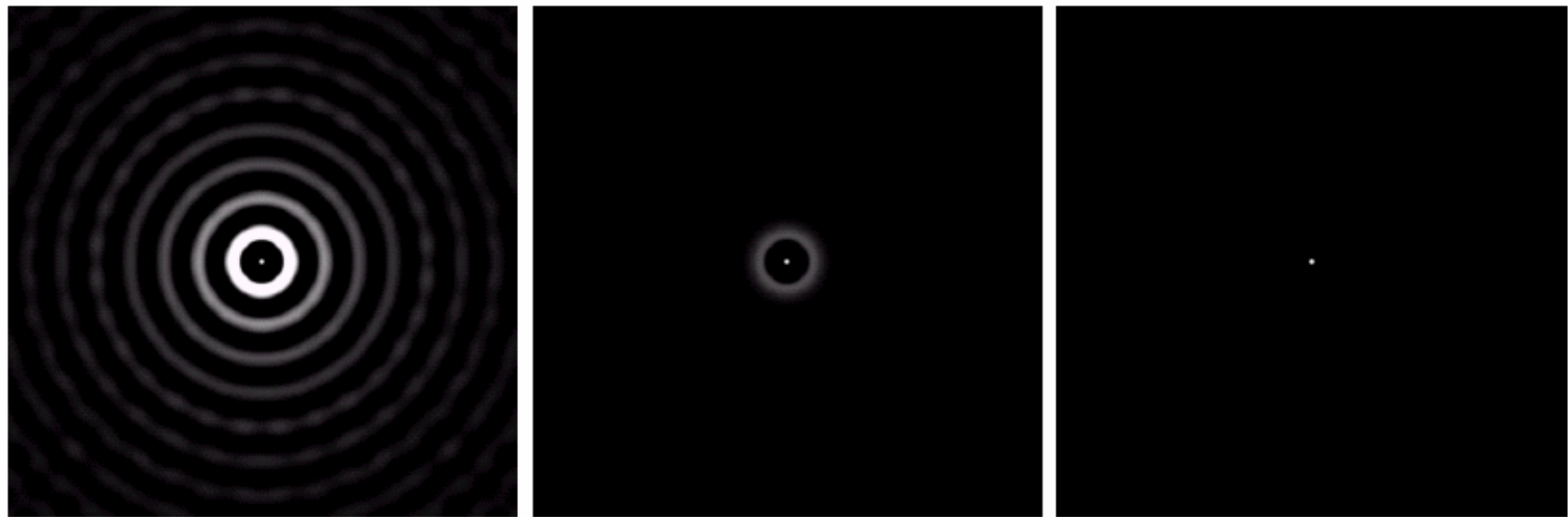
a b c  
d e f  
g h i

FIGURE 4.22 Top row: Perspective plot, image representation, and cross section of a typical ideal highpass filter. Middle and bottom rows: The same sequence for typical Butterworth and Gaussian highpass filters.



## 4.4 Sharpening Frequency-Domain Filters

- Highpass Filtering
  - [Fig. 4.22](#)
  - [Fig. 4.23](#)
  - Ideal highpass filters
    - [Fig. 4.24](#)
  - Butterworth highpass filters
    - [Fig. 4.25](#)
  - Gaussian highpass filters
    - [Fig. 4.26](#)



a b c

**FIGURE 4.23** Spatial representations of typical (a) ideal, (b) Butterworth, and (c) Gaussian frequency domain highpass filters, and corresponding gray-level profiles.



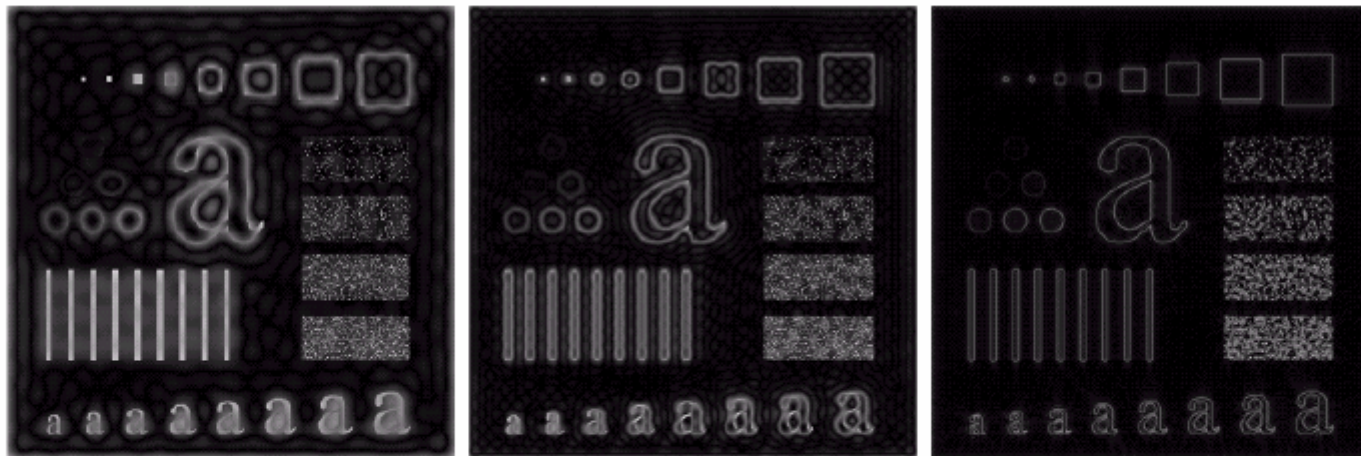
# Ideal highpass filters

$$H(u, v) = \begin{cases} 0 & \text{if } D(u, v) \leq D_0 \\ 1 & \text{if } D(u, v) > D_0 \end{cases}$$



$$H(u, v) = \begin{cases} 1 & \text{if } D(u, v) \leq D_0 \\ 0 & \text{if } D(u, v) > D_0 \end{cases}$$

ILPF



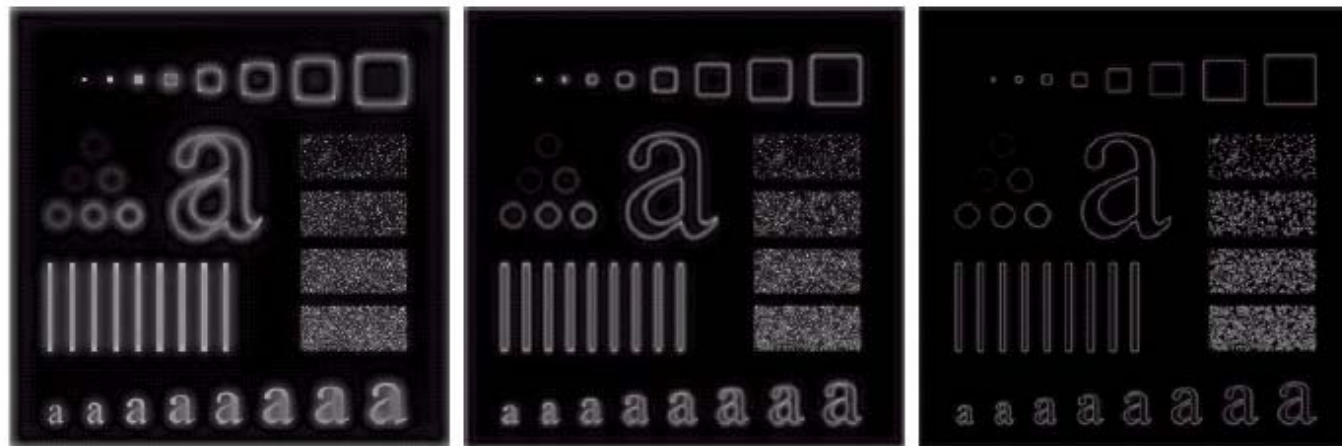
a b c

**FIGURE 4.24** Results of ideal highpass filtering the image in Fig. 4.11(a) with  $D_0 = 15, 30,$  and  $80,$  respectively. Problems with ringing are quite evident in (a) and (b).

## Butterworth highpass filters

$$H(u,v) = 1 - \frac{1}{1 + [D(u,v)/D_0]^{2n}} = \frac{[D(u,v)/D_0]^{2n}}{1 + [D(u,v)/D_0]^{2n}} = \frac{1}{1 + [D_0/D(u,v)]^{2n}}$$

$$H(u,v) = \frac{1}{1 + [D_0/D(u,v)]^{2n}}$$

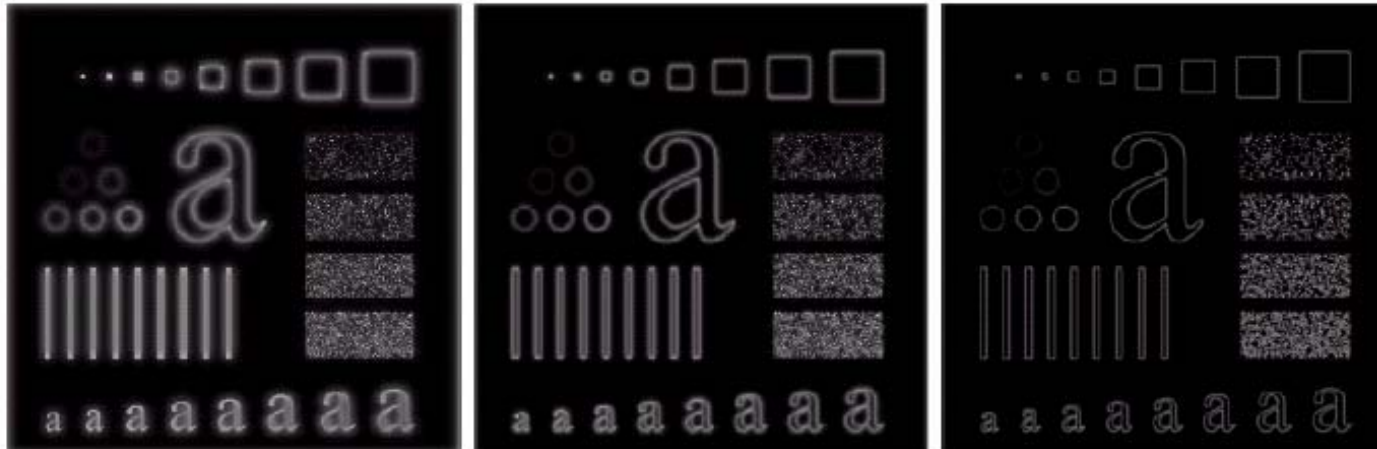


a b c

**FIGURE 4.25** Results of highpass filtering the image in Fig. 4.11(a) using a BHPF of order 2 with  $D_0 = 15$ , 30, and 80, respectively. These results are much smoother than those obtained with an ILPF.

## Gaussian highpass filters

$$H(u, v) = 1 - e^{-D^2(u, v) / 2D_0^2}$$



a b c

**FIGURE 4.26** Results of highpass filtering the image of Fig. 4.11(a) using a GHPF of order 2 with  $D_0 = 15$ , 30, and 80, respectively. Compare with Figs. 4.24 and 4.25.



## 4.4 Sharpening Frequency-Domain Filters

- The Laplacian in the frequency domain
  - [Fig. 4.27](#)
  - Example 4.7: Laplacian ([Fig. 4.28](#))
- Unsharp masking, High-boost filtering, and High-frequency emphasis filtering
  - Example 4.8: ([Fig. 4.29](#))
  - Example 4.9: ([Fig. 4.30](#))





# Laplacian in the frequency domain

$$\mathfrak{F} \left[ \frac{d^n f(x)}{dx^n} \right] = (j2\pi u)^n F(u)$$

$$\mathfrak{F} \{f(x)\} = F(u) = \int_{-\infty}^{\infty} f(x) \exp[-j2\pi ux] dx$$

$$\mathfrak{F}^{-1} \{F(u)\} = f(x) = \int_{-\infty}^{\infty} F(u) \exp[j2\pi ux] du$$

$$\mathfrak{F} \left[ \frac{\partial^2 f(x, y)}{\partial x^2} + \frac{\partial^2 f(x, y)}{\partial y^2} \right] = (j2\pi u)^2 F(u, v) + (j2\pi v)^2 F(u, v) = -4\pi^2 (u^2 + v^2) F(u, v)$$

$$H(u, v) = -4\pi^2 (u^2 + v^2)$$

$$\mathfrak{F} \{f(x, y)\} = F(u, v) = \iint f(x, y) \exp[-j2\pi(ux + vy)] dx dy$$

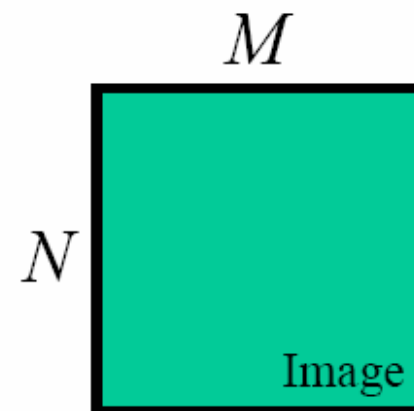
$$\mathfrak{F}^{-1} \{F(u, v)\} = f(x, y) = \iint F(u, v) \exp[j2\pi(ux + vy)] du dv$$

$$H(u, v) = - \left[ (u - M/2)^2 + (v - N/2)^2 \right]$$

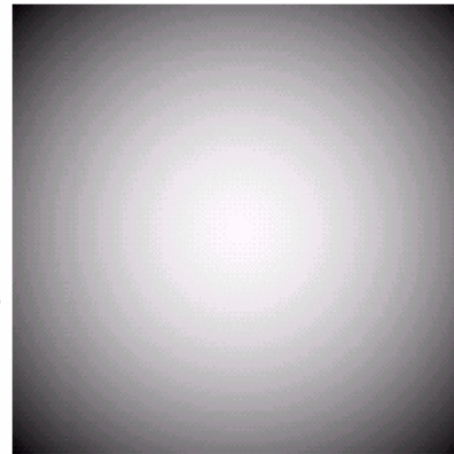
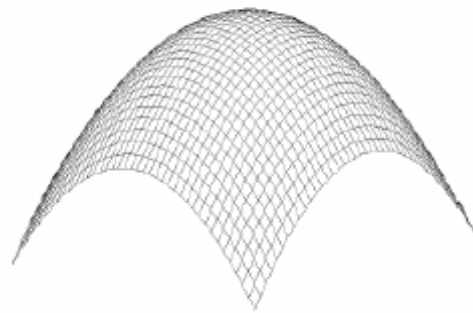
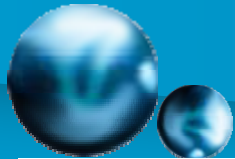
$$\nabla^2 f(x, y) = \mathfrak{F}^{-1} \left\{ - \left[ (u - M/2)^2 + (v - N/2)^2 \right] F(u, v) \right\}$$

$$F(u, v) = \frac{1}{MN} \sum_{x=0}^{M-1} \sum_{y=0}^{N-1} f(x, y) e^{-j\frac{2\pi ux}{N}} e^{-j\frac{2\pi vy}{N}}, u = 0, 1, \dots, M-1, v = 0, 1, \dots, N-1$$

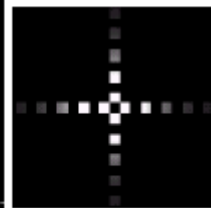
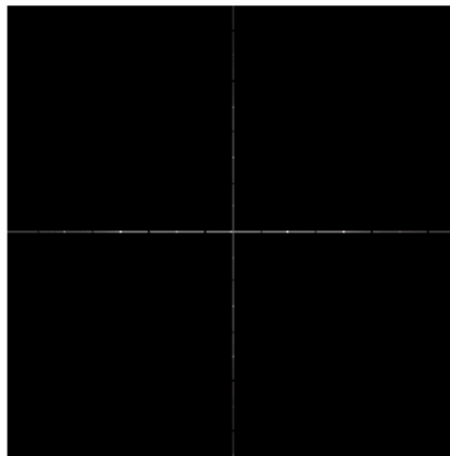
$$f(x, y) = \sum_{u=0}^{M-1} \sum_{v=0}^{N-1} F(u, v) e^{j\frac{2\pi ux}{N}} e^{j\frac{2\pi vy}{N}}, x = 0, 1, \dots, M-1, y = 0, 1, \dots, N-1$$







$$H(u, v) = -\left[ (u - M/2)^2 + (v - N/2)^2 \right]$$

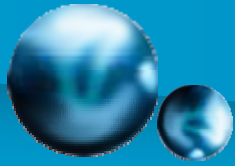


0	1	0
1	-4	1
0	1	0

a b  
c d e  
f

**FIGURE 4.27** (a) 3-D plot of Laplacian in the frequency domain. (b) Image representation of (a). (c) Laplacian in the spatial domain obtained from the inverse DFT of (b). (d) Zoomed section of the origin of (c). (e) Gray-level profile through the center of (d). (f) Laplacian mask used in Section 3.7.

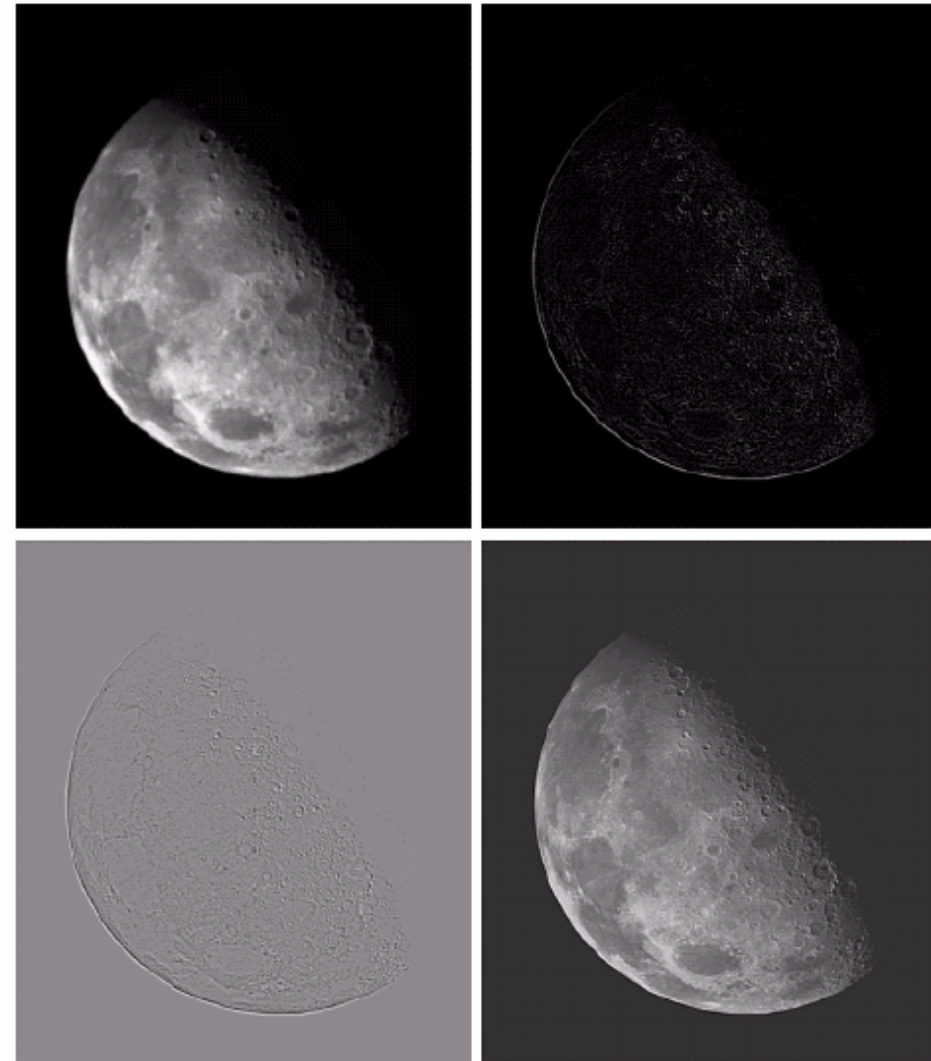




$$g(x, y) = f(x, y) - \nabla^2 f(x, y)$$

a	b
c	d

**FIGURE 4.28**  
 (a) Image of the North Pole of the moon.  
 (b) Laplacian filtered image.  
 (c) Laplacian image scaled.  
 (d) Image enhanced by using Eq. (4.4-12).  
 (Original image courtesy of NASA.)



$$H(u, v) = 1 - \left[ (u - M/2)^2 + (v - N/2)^2 \right]$$

$$g(x, y) = \mathfrak{F}^{-1} \left\{ \left[ 1 - \left( (u - M/2)^2 + (v - N/2)^2 \right) \right] F(u, v) \right\}$$



# High-boost filtering

$$f_s(x, y) = f(x, y) - \bar{f}(x, y)$$

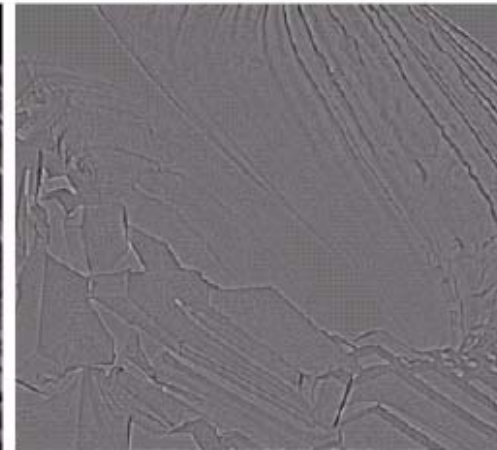
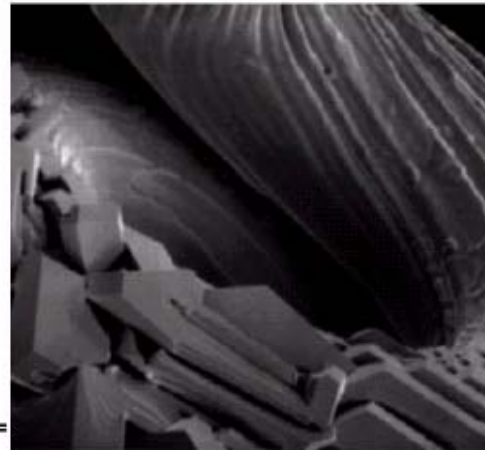
$$f_{lp}(x, y) = f(x, y) - f_{hp}(x, y)$$

$$H_{lp}(u, v) = 1 - H_{hp}(u, v)$$

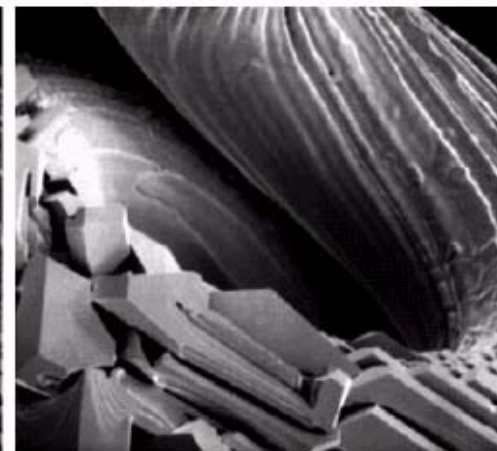
$$f_{hb}(x, y) = Af(x, y) - f_{lp}(x, y)$$

$$\begin{aligned} f_{hb}(x, y) &= (A-1)f(x, y) + f(x, y) - f_{lp}(x, y) \\ &= (A-1)f(x, y) + f_{lp}(x, y) \end{aligned}$$

$$H_{hb}(u, v) = (A-1) + H_{lp}(u, v)$$



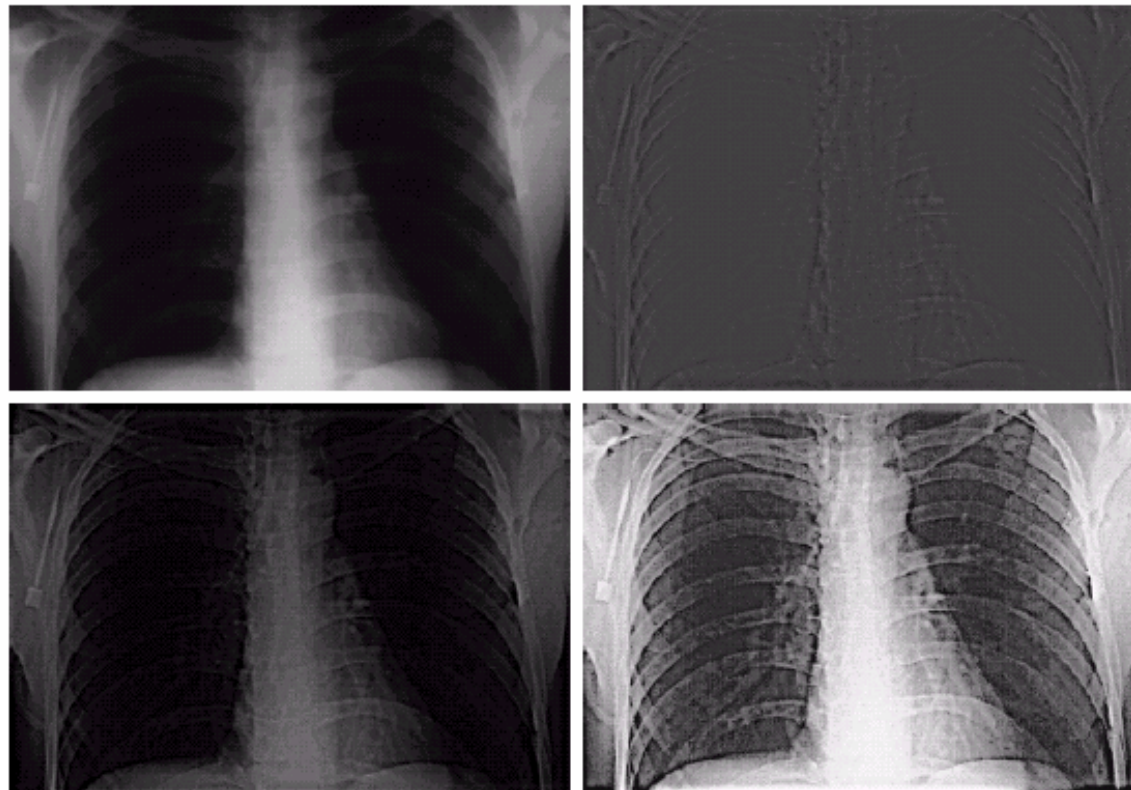
A=2



A=2.6

# High-frequency emphasis filtering

$$H_{\text{hfe}}(u, v) = a + bH_{\text{hp}}(u, v) \quad a \geq 0 \text{ and } b > a$$



a	b
c	d

**FIGURE 4.30**

(a) A chest X-ray image. (b) Result of Butterworth highpass filtering. (c) Result of high-frequency emphasis filtering. (d) Result of performing histogram equalization on (c). (Original image courtesy Dr. Thomas R. Gest, Division of Anatomical Sciences, University of Michigan Medical School.)

$$a = 0.5$$

$$b = 2.0$$

# Homomorphic Filtering

illumination      reflectance

$$f(x, y) = i(x, y) \cdot r(x, y) \longrightarrow \mathfrak{T}\{f(x, y)\} \neq \mathfrak{T}\{i(x, y)\} \cdot \mathfrak{T}\{r(x, y)\}$$

$$z(x, y) = \ln f(x, y) = \ln i(x, y) + \ln r(x, y)$$

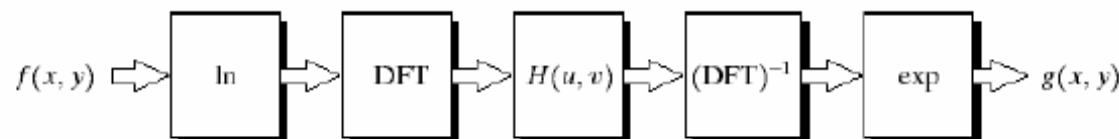
$$\mathfrak{T}\{z(x, y)\} = \mathfrak{T}\{\ln f(x, y)\} = \mathfrak{T}\{\ln i(x, y)\} + \mathfrak{T}\{\ln r(x, y)\}$$

$$Z(u, v) = F_i(u, v) + F_r(u, v)$$

$$S(u, v) = H(u, v)Z(u, v) = H(u, v)F_i(u, v) + H(u, v)F_r(u, v)$$

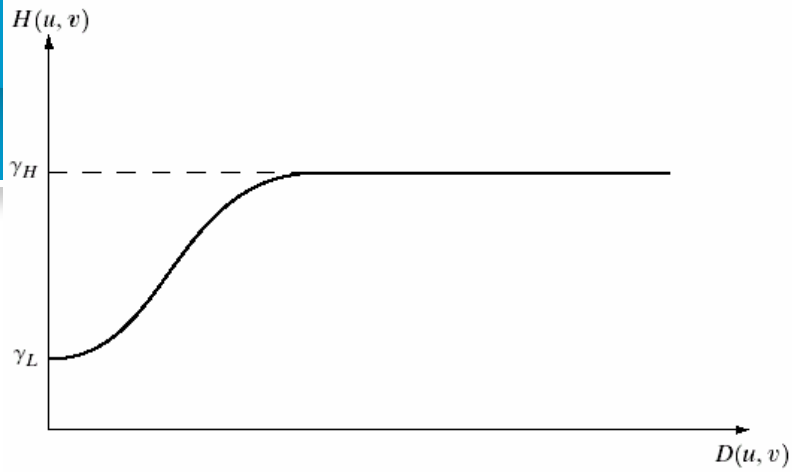
$$s(x, y) = \mathfrak{T}^{-1}\{S(u, v)\} = \mathfrak{T}^{-1}\{H(u, v)F_i(u, v)\} + \mathfrak{T}^{-1}\{H(u, v)F_r(u, v)\} = i'(x, y) + r'(x, y)$$

$$g(x, y) = e^{s(x, y)} = e^{i'(x, y)} \cdot e^{r'(x, y)} = i_0(x, y) \cdot r_0(x, y)$$



**FIGURE 4.31**  
Homomorphic  
filtering approach  
for image  
enhancement.

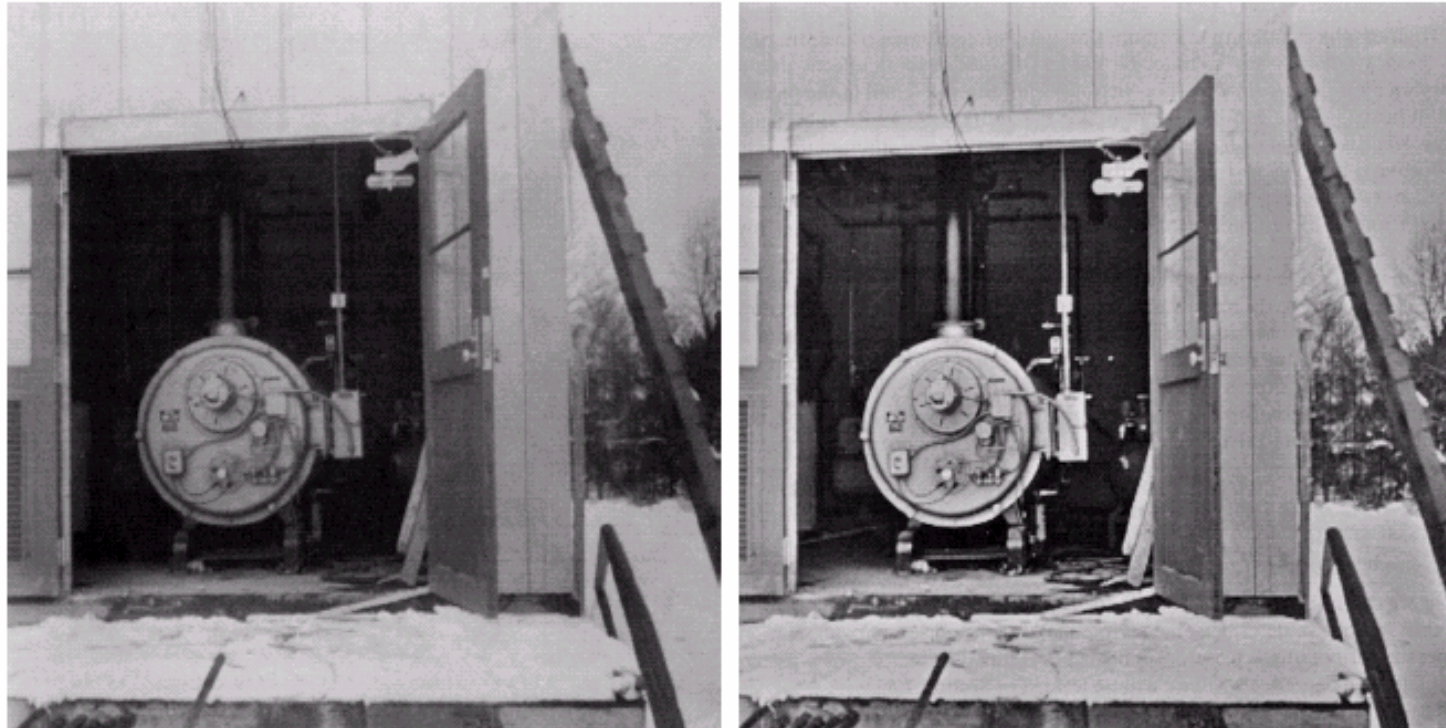


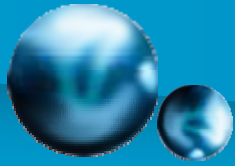


**FIGURE 4.32**  
Cross section of a circularly symmetric filter function.  $D(u, v)$  is the distance from the origin of the centered transform.

a b

**FIGURE 4.33**  
(a) Original image. (b) Image processed by homomorphic filtering (note details inside shelter). (Stockham.)

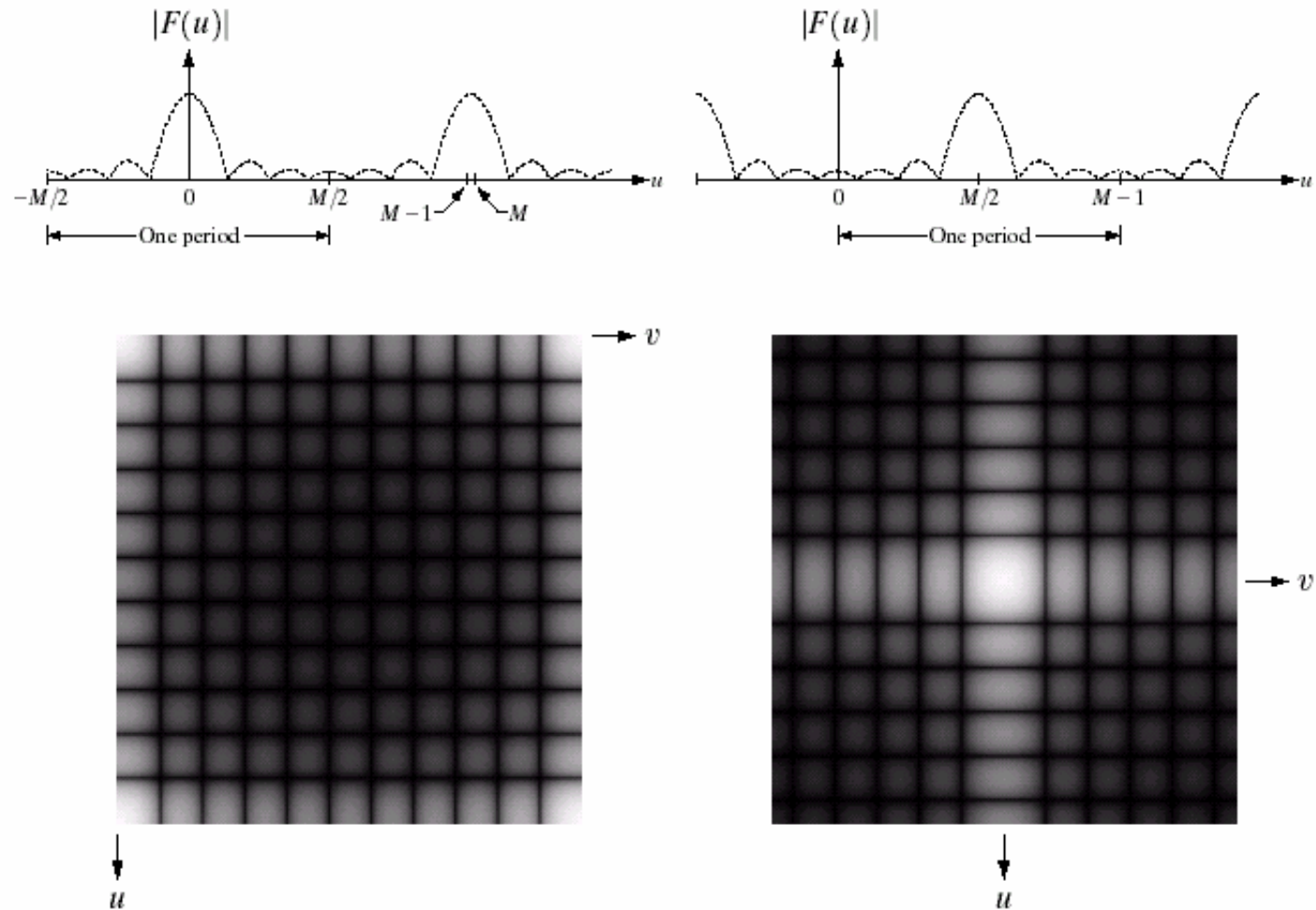




a b  
c d

**FIGURE 4.34**

(a) Fourier spectrum showing back-to-back half periods in the interval  $[0, M - 1]$ .  
 (b) Shifted spectrum showing a full period in the same interval.  
 (c) Fourier spectrum of an image, showing the same back-to-back properties as (a), but in two dimensions.  
 (d) Centered Fourier spectrum.





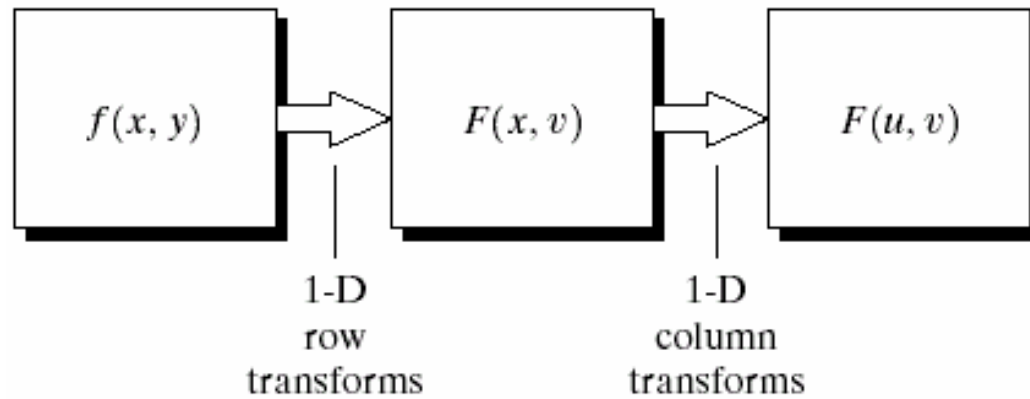
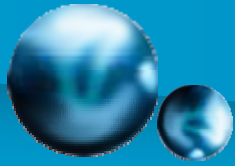


**FIGURE 4.35**  
Computation of the 2-D Fourier transform as a series of 1-D transforms.



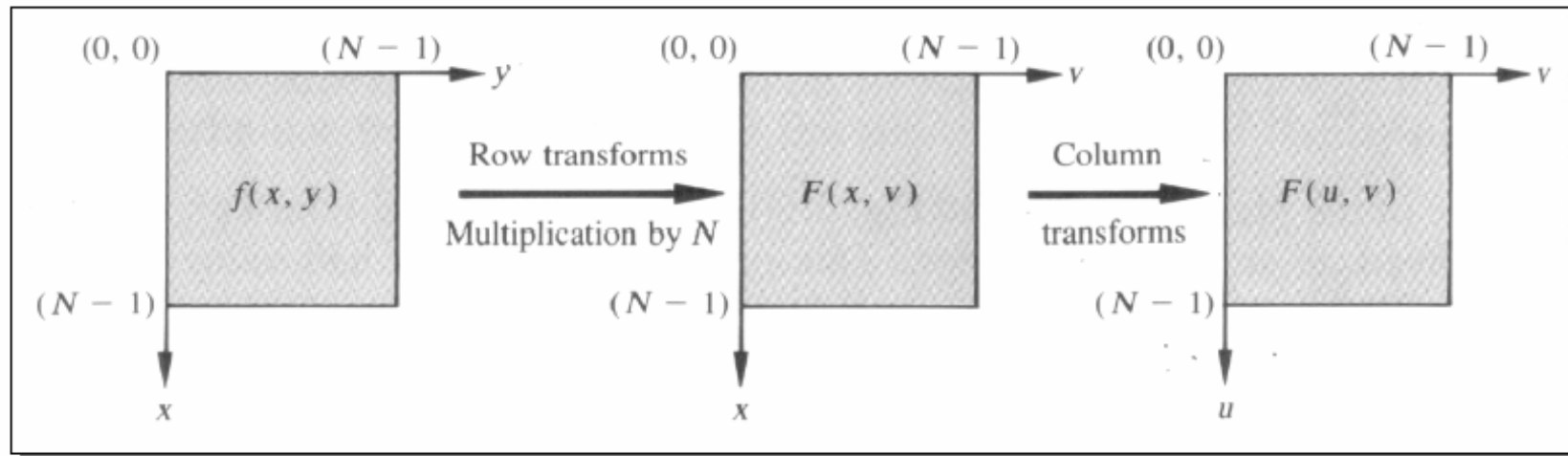
## 4.2 Introduction to the Fourier transform

✓ The 2-D DFT Calculation with two 1-D DFT:

$$F(u, v) = \frac{1}{N} \sum_{x=0}^{N-1} \sum_{y=0}^{N-1} f(x, y) W_N^{ux} W_N^{vy}$$

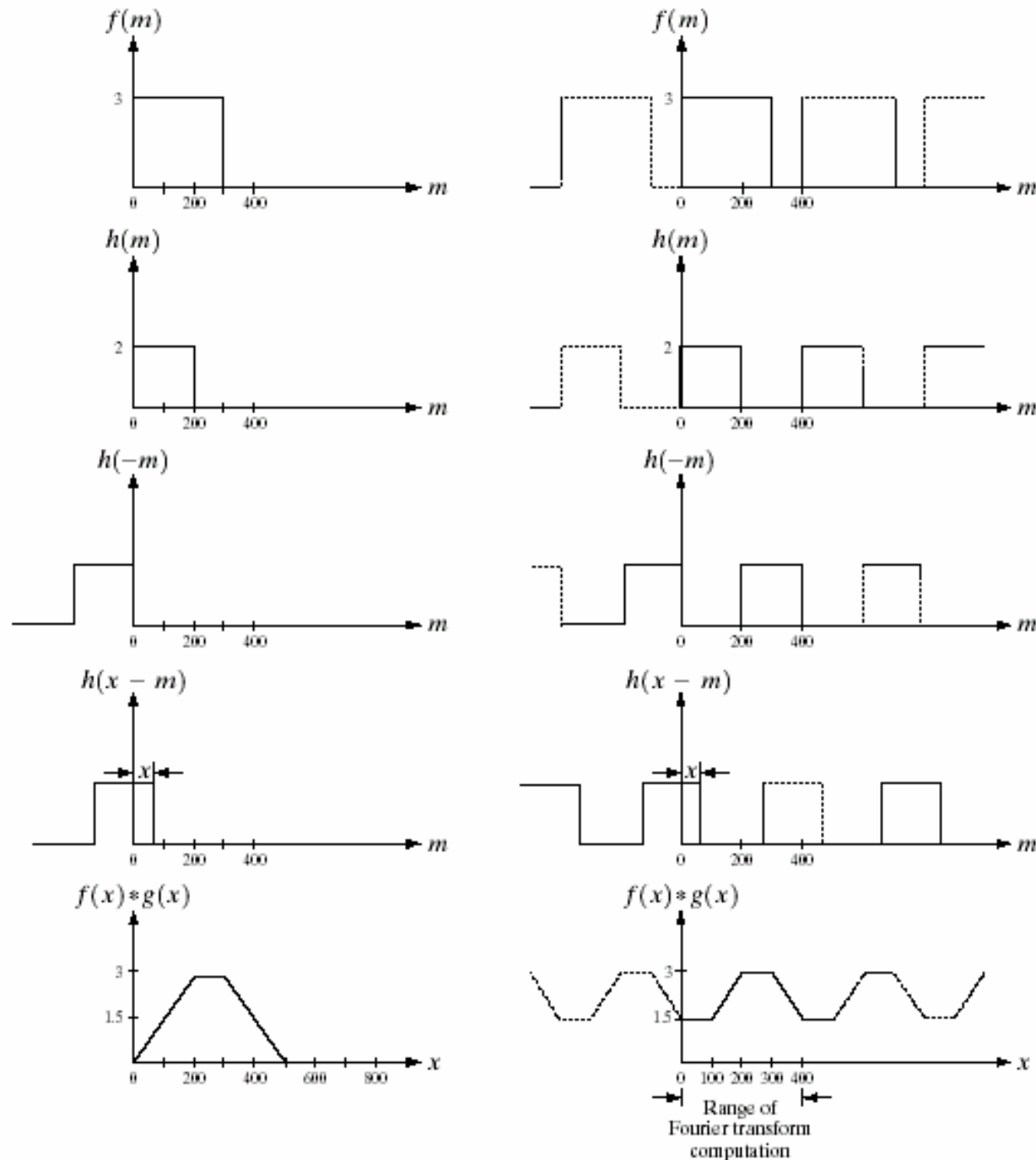
$$\Rightarrow F(x, v) = \frac{1}{N} \sum_{y=0}^{N-1} f(x, y) W_N^{vy}$$

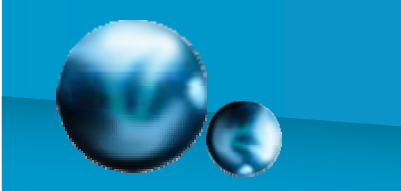
$$\Rightarrow F(u, v) = N \left( \frac{1}{N} \sum_{x=0}^{N-1} F(x, v) W_N^{ux} \right)$$



a	f
b	g
c	h
d	i
e	j

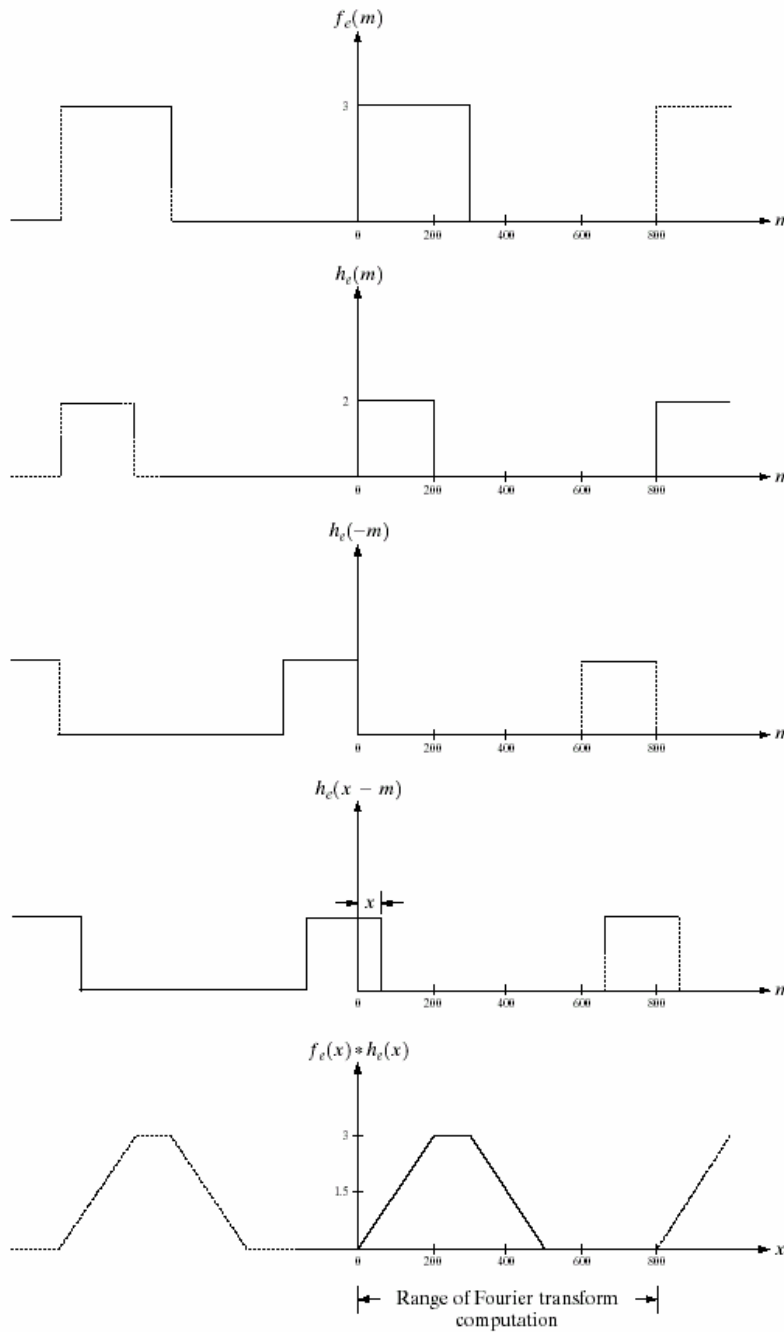
**FIGURE 4.36** Left: convolution of two discrete functions. Right: convolution of the same functions, taking into account the implied periodicity of the DFT. Note in (j) how data from adjacent periods corrupt the result of convolution.

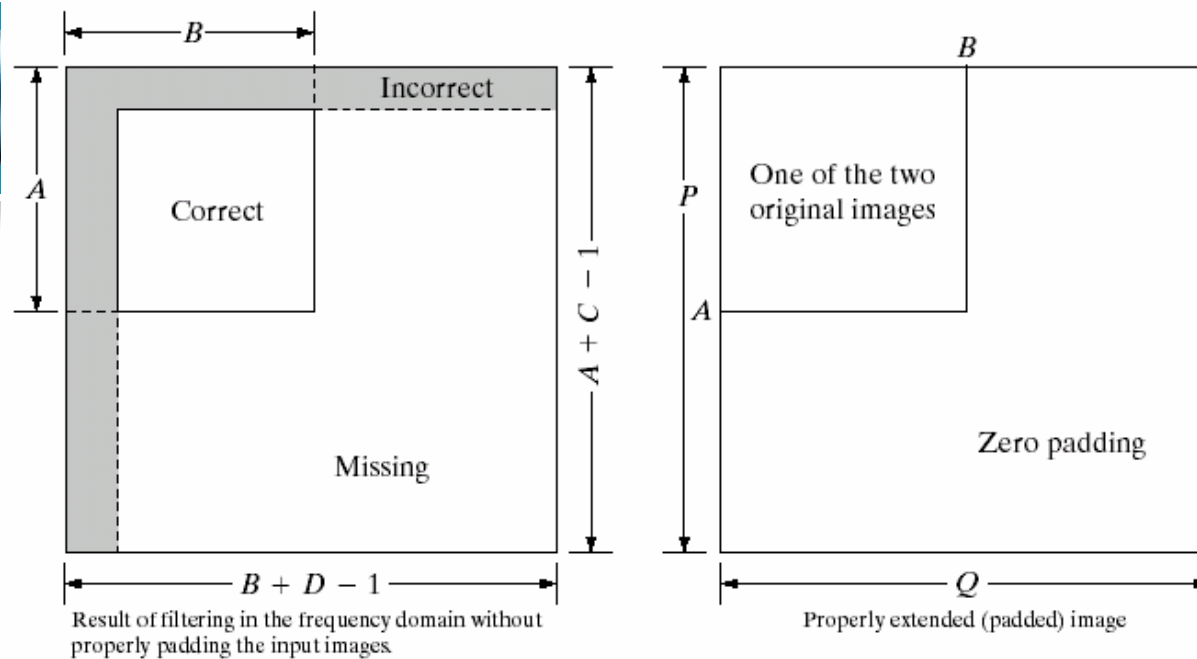
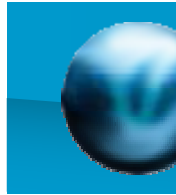




a  
b  
c  
d  
e

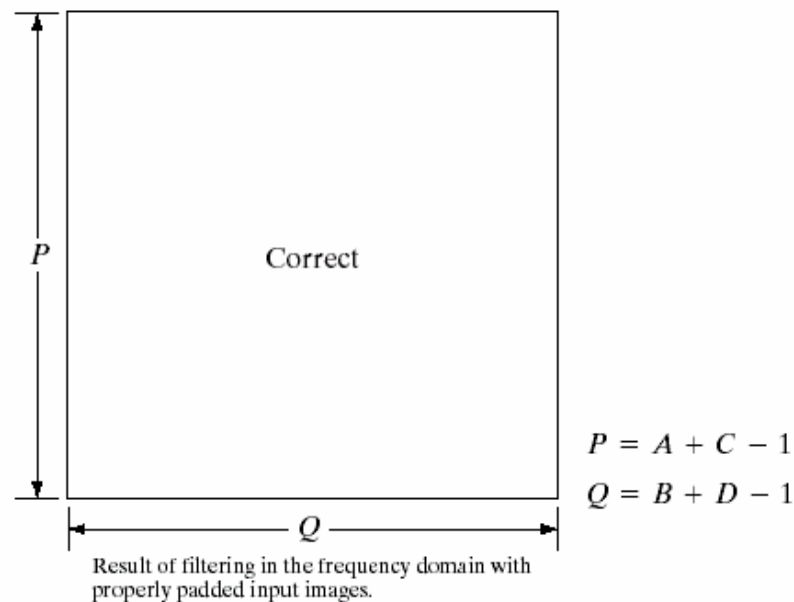
**FIGURE 4.37**  
Result of performing convolution with extended functions. Compare Figs. 4.37(e) and 4.36(e).





a b  
c

**FIGURE 4.38** Illustration of the need for function padding. (a) Result of performing 2-D convolution without padding. (b) Proper function padding. (c) Correct convolution result.



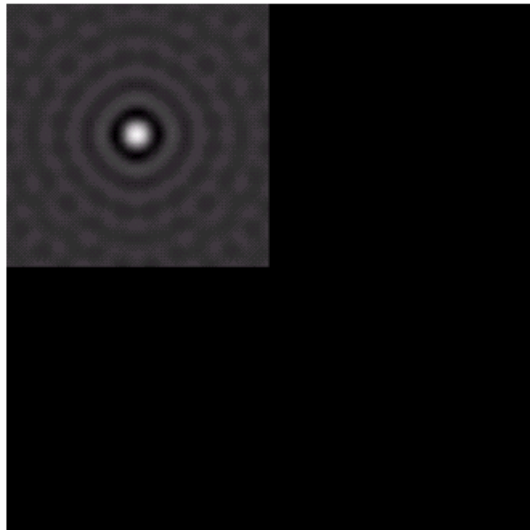
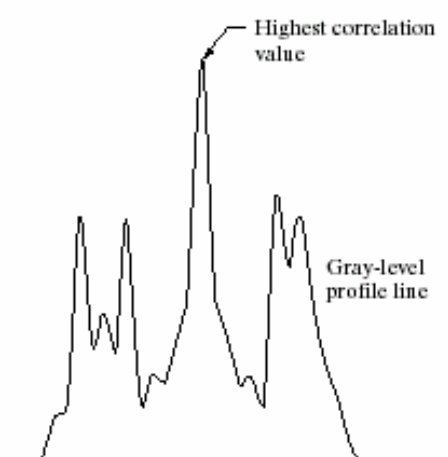
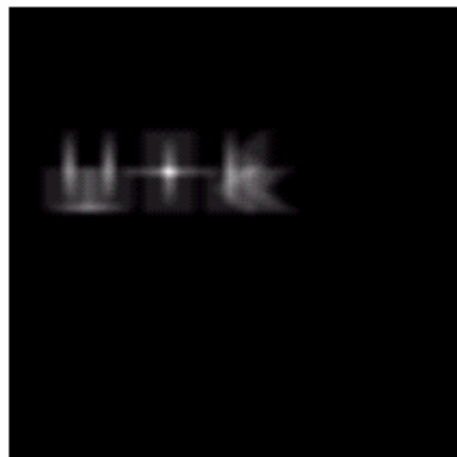
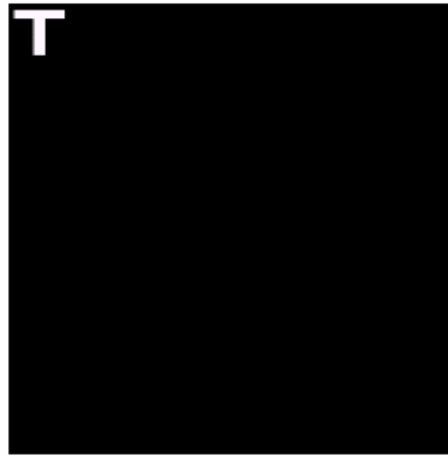
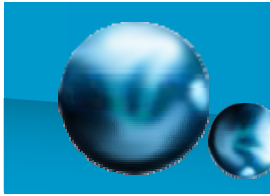


**FIGURE 4.39** Padded lowpass filter in the spatial domain (only the real part is shown).



**FIGURE 4.40** Result of filtering with padding. The image is usually cropped to its original size since there is little valuable information past the image boundaries.



a b  
c d  
e f

**FIGURE 4.41**

(a) Image.  
(b) Template.  
(c) and  
(d) Padded  
images.  
(e) Correlation  
function displayed  
as an image.  
(f) Horizontal  
profile line  
through the  
highest value in  
(e), showing the  
point at which the  
best match took  
place.





**TABLE 4.1**

Summary of some important properties of the 2-D Fourier transform.

Property	Expression(s)
Fourier transform	$F(u, v) = \frac{1}{MN} \sum_{x=0}^{M-1} \sum_{y=0}^{N-1} f(x, y) e^{-j2\pi(ux/M+vy/N)}$
Inverse Fourier transform	$f(x, y) = \sum_{u=0}^{M-1} \sum_{v=0}^{N-1} F(u, v) e^{j2\pi(ux/M+vy/N)}$
Polar representation	$F(u, v) =  F(u, v)  e^{-j\phi(u, v)}$
Spectrum	$ F(u, v)  = [R^2(u, v) + I^2(u, v)]^{1/2}, \quad R = \text{Real}(F) \text{ and } I = \text{Imag}(F)$
Phase angle	$\phi(u, v) = \tan^{-1} \left[ \frac{I(u, v)}{R(u, v)} \right]$
Power spectrum	$P(u, v) =  F(u, v) ^2$
Average value	$\bar{f}(x, y) = F(0, 0) = \frac{1}{MN} \sum_{x=0}^{M-1} \sum_{y=0}^{N-1} f(x, y)$
Translation	$f(x, y) e^{j2\pi(u_0x/M+v_0y/N)} \Leftrightarrow F(u - u_0, v - v_0)$ $f(x - x_0, y - y_0) \Leftrightarrow F(u, v) e^{-j2\pi(ux_0/M+vy_0/N)}$ <p>When <math>x_0 = u_0 = M/2</math> and <math>y_0 = v_0 = N/2</math>, then</p> $f(x, y) (-1)^{x+y} \Leftrightarrow F(u - M/2, v - N/2)$ $f(x - M/2, y - N/2) \Leftrightarrow F(u, v) (-1)^{u+v}$



Conjugate symmetry	$F(u, v) = F^*(-u, -v)$ $ F(u, v)  =  F(-u, -v) $
Differentiation	$\frac{\partial^n f(x, y)}{\partial x^n} \Leftrightarrow (ju)^n F(u, v)$ $(-jx)^n f(x, y) \Leftrightarrow \frac{\partial^n F(u, v)}{\partial u^n}$
Laplacian	$\nabla^2 f(x, y) \Leftrightarrow -(u^2 + v^2)F(u, v)$
Distributivity	$\mathfrak{F}[f_1(x, y) + f_2(x, y)] = \mathfrak{F}[f_1(x, y)] + \mathfrak{F}[f_2(x, y)]$ $\mathfrak{F}[f_1(x, y) \cdot f_2(x, y)] \neq \mathfrak{F}[f_1(x, y)] \cdot \mathfrak{F}[f_2(x, y)]$
Scaling	$af(x, y) \Leftrightarrow aF(u, v), f(ax, by) \Leftrightarrow \frac{1}{ ab } F(u/a, v/b)$
Rotation	$x = r \cos \theta \quad y = r \sin \theta \quad u = \omega \cos \varphi \quad v = \omega \sin \varphi$ $f(r, \theta + \theta_0) \Leftrightarrow F(\omega, \varphi + \theta_0)$
Periodicity	$F(u, v) = F(u + M, v) = F(u, v + N) = F(u + M, v + N)$ $f(x, y) = f(x + M, y) = f(x, y + N) = f(x + M, y + N)$
Separability	<p>See Eqs. (4.6-14) and (4.6-15). Separability implies that we can compute the 2-D transform of an image by first computing 1-D transforms along each row of the image, and then computing a 1-D transform along each column of this intermediate result. The reverse, columns and then rows, yields the same result.</p>

**TABLE 4.1**  
(continued)

**TABLE 4.1**  
(continued)

Property	Expression(s)
Computation of the inverse Fourier transform using a forward transform algorithm	$\frac{1}{MN} f^*(x, y) = \frac{1}{MN} \sum_{u=0}^{M-1} \sum_{v=0}^{N-1} F^*(u, v) e^{-j2\pi(ux/M + vy/N)}$ <p>This equation indicates that inputting the function <math>F^*(u, v)</math> into an algorithm designed to compute the forward transform (right side of the preceding equation) yields <math>f^*(x, y)/MN</math>. Taking the complex conjugate and multiplying this result by <math>MN</math> gives the desired inverse.</p>
Convolution <sup>†</sup>	$f(x, y) * h(x, y) = \frac{1}{MN} \sum_{m=0}^{M-1} \sum_{n=0}^{N-1} f(m, n) h(x - m, y - n)$
Correlation <sup>†</sup>	$f(x, y) \circ h(x, y) = \frac{1}{MN} \sum_{m=0}^{M-1} \sum_{n=0}^{N-1} f^*(m, n) h(x + m, y + n)$
Convolution theorem <sup>†</sup>	$f(x, y) * h(x, y) \Leftrightarrow F(u, v) H(u, v);$ $f(x, y) h(x, y) \Leftrightarrow F(u, v) * H(u, v)$
Correlation theorem <sup>†</sup>	$f(x, y) \circ h(x, y) \Leftrightarrow F^*(u, v) H(u, v);$ $f^*(x, y) h(x, y) \Leftrightarrow F(u, v) \circ H(u, v)$



**TABLE 4.1**  
(continued)

Some useful FT pairs:

*Impulse*             $\delta(x, y) \Leftrightarrow 1$

*Gaussian*             $A\sqrt{2\pi}\sigma e^{-2\pi^2\sigma^2(x^2+y^2)} \Leftrightarrow Ae^{-(u^2+v^2)/2\sigma^2}$

*Rectangle*             $\text{rect}[a, b] \Leftrightarrow ab \frac{\sin(\pi ua)}{(\pi ua)} \frac{\sin(\pi vb)}{(\pi vb)} e^{-j\pi(ua+vb)}$

*Cosine*             $\cos(2\pi u_0 x + 2\pi v_0 y) \Leftrightarrow$   
 $\frac{1}{2} [\delta(u + u_0, v + v_0) + \delta(u - u_0, v - v_0)]$

*Sine*             $\sin(2\pi u_0 x + 2\pi v_0 y) \Leftrightarrow$   
 $j \frac{1}{2} [\delta(u + u_0, v + v_0) - \delta(u - u_0, v - v_0)]$

† Assumes that functions have been extended by zero padding.

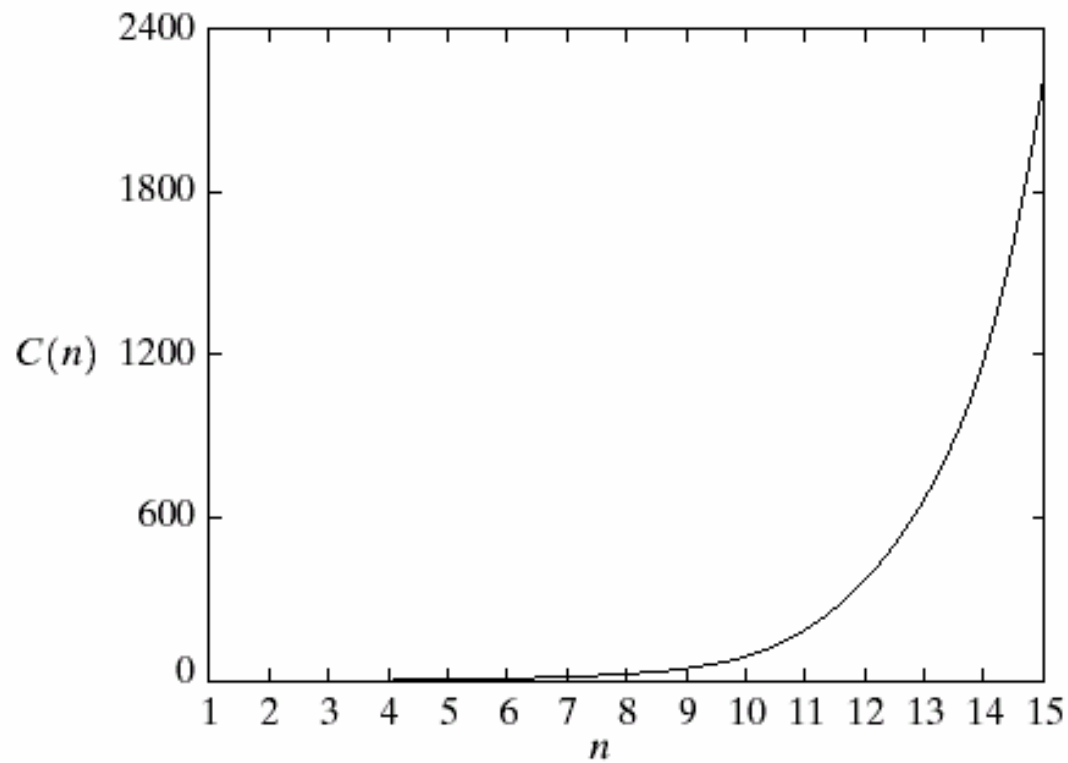
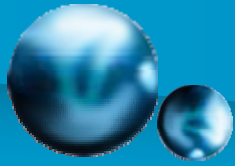


**FIGURE 4.42**  
Computational advantage of the FFT over a direct implementation of the 1-D DFT. Note that the advantage increases rapidly as a function of  $n$ .